Received: 18 December 2016 | Revised: 8 February 2017 | Accepted: 9 February 2017

DOI 10.1002/cne.24195

RESEARCH ARTICLE

WILEY The Journal of Comparative Neurology

The Centrifugal visual system of a palaeognathous bird, the Chilean Tinamou (*Nothoprocta perdicaria*)

Quirin Krabichler[1] | Tomas Vega-Zuniga[1] | Denisse Carrasco[2] | Maximo Fernandez[2] | Cristián Gutiérrez-Ibáñez[1] | Gonzalo Marín[2,3]* | Harald Luksch[1]*

[1]Lehrstuhl für Zoologie, Technische Universität München, Freising-Weihenstephan, Germany

[2]Departamento de Biología, Facultad de Ciencias, Universidad de Chile, Santiago, Chile

[3]Facultad de Medicina, Universidad Finis Terrae, Santiago, Chile

Correspondence: Quirin Krabichler, Lehrstuhl für Zoologie, Technische Universität München, Liesel-Beckmann Strasse 4, 85354 Freising-Weihenstephan, Germany.
E-mail: quirin.krabichler@tum.de

Funding information: Bernstein Center for Computational Neuroscience (BCCN) Munich (H.L.), Grant/Award Number: FKZ01GQ1004B; FONDECYT (G.M.), Grant/Award Number: #1151432.

Abstract

The avian centrifugal visual system, which projects from the brain to the retina, has been intensively studied in several Neognathous birds that have a distinct isthmo-optic nucleus (ION). However, birds of the order Palaeognathae seem to lack a proper ION in histologically stained brain sections. We had previously reported in the palaeognathous Chilean Tinamou (*Nothoprocta perdicaria*) that intraocular injections of Cholera Toxin B subunit retrogradely label a considerable number of neurons, which form a diffuse isthmo-optic complex (IOC). In order to better understand how this IOC-based centrifugal visual system is organized, we have studied its major components by means of in vivo and in vitro tracing experiments. Our results show that the IOC, though structurally less organized than an ION, possesses a dense core region consisting of multipolar neurons. It receives afferents from neurons in L10a of the optic tectum, which are distributed with a wider interneuronal spacing than in Neognathae. The tecto-IOC terminals are delicate and divergent, unlike the prominent convergent tecto-ION terminals in Neognathae. The centrifugal IOC terminals in the retina are exclusively divergent, resembling the terminals from "ectopic" centrifugal neurons in Neognathae. We conclude that the Tinamou's IOC participates in a comparable general IOC-retina-TeO-IOC circuitry as the neognathous ION. However, the connections between the components are structurally different and their divergent character suggests a lower spatial resolution. Our findings call for further comparative studies in a broad range of species for advancing our understanding of the evolution, plasticity and functional roles of the avian centrifugal visual system.

KEYWORDS

isthmo-optic nucleus, ectopic centrifugal neurons, retinopetal, divergent terminals, optic tectum, tecto-isthmal, association amacrine cells, tyramide signal amplification, RRID:AB_10013220, RRID:AB_2315144, RRID:AB_477329, RRID:AB_2336126, RRID:AB_2534088

1 | INTRODUCTION

The visual system is generally thought of in terms of feed-forward pathways from the retina to the brain. However, after Santiago Ramón y Cajal first demonstrated terminal endings in the retina of birds (Ramón y Cajal, 1889), a brain-to-retina feed-back projection called centrifugal visual system has been found in all major vertebrate taxa. While the neuroanatomical location of the centrifugal visual neurons can be surprisingly diverse among different vertebrates (reviewed in Repérant, Miceli, Vesselkin, & Molotchnikoff, 1989; Repérant et al.

Abbreviations: AAC, association amacrine cell; BDA, biotinylated dextran amine, 3 kDa; CTB, Cholera toxin B subunit; DAB, diaminobenzidine; FRL, formatio reticularis lateralis; Imc, nucleus isthmi, pars magnocellularis; INL, inner nuclear layer; IO, isthmo-optic; IOC, isthmo-optic complex; ION, isthmo-optic nucleus; IV, trochlear nucleus; Ipc, nucleus isthmi, pars parvocellularis; IPL, inner plexiform layer; LLD, dorsal nucleus of the lateral lemniscus; MLd, nucleus mesencephalicus lateralis, pars dorsalis; nIV, trochlear nerve; PHAL, *Phaseolus vulgaris* leucoagglutinin; RITC, Rhodamine B isothiocyanate; RT, room temperature; tecto-IO, tecto-isthmo-optic; TeO, optic tectum; TIO, isthmo-optic tract; TSA, tyramide signal amplification.

*Gonzalo Marín and Harald Luksch are co-senior authors.

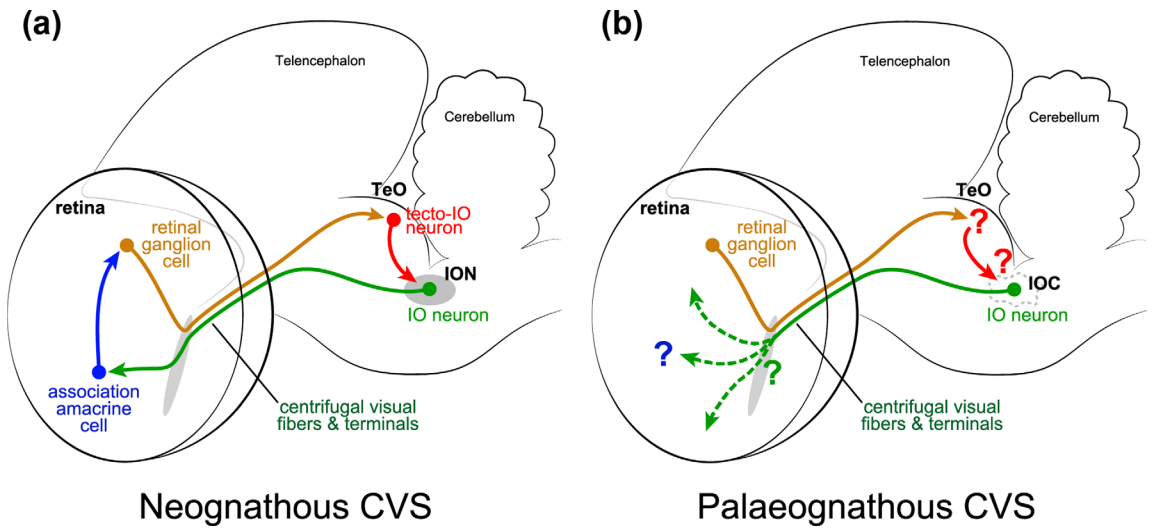

FIGURE 1 Schematic of the centrifugal visual system circuitry in birds. (a) In Neognathae, the isthmo-optic nucleus (ION) is an organized isthmic structure that receives a topographic projection from the optic tectum (TeO). The IO neurons project to the ventral half of the contralateral retina, where they synapse on specific target cells in the inner nuclear layer (INL), called "association amacrine cells" (AACs). These are axon-bearing and are thought to project to ganglion cells in other parts of the retina. Tectofugal ganglion cells send axons to the TeO, which contact the L9-neurons projecting to the ION. (b) In Palaeognathae, the IO neurons form a diffuse structure (isthmo-optic complex, IOC) at a comparable location as the Neognathous ION. The circuitry in which these neurons participate has so far not been studied. Schematic adapted from "Lesion of the isthmo-optic nucleus impairs target selection for visually guided reaching" by Uchiyama, Ohno, & Kodama, 2012, Behavioural Brain Research, 233, 359-366 [Color figure can be viewed at wileyonlinelibrary.com]

2006, 2007), in nonmammalian amniotes these cells are found in the isthmus, the junction between mid and hindbrain (Repérant et al., 2006).

The centrifugal visual system of neognathous birds (Figure 1a) generally contains the largest number of such cells and has therefore received much attention (Repérant et al., 1989; Uchiyama, 1989; Wilson & Lindstrom, 2011). Most of their centrifugal visual neurons constitute the isthmo-optic nucleus (ION; Cowan, Adamson, & Powell, 1961), which is conspicuously organized as a convoluted lamina of cells around a central dendritic neuropil (McGill, Powell, & Cowan, 1966a, 1966b). The main afferents to the ION originate from a distinct population of tecto-isthmo-optic (tecto-ION) neurons in L9-10 of the ipsilateral TeO, which project topographically upon the ION (Holden, 1968), and have been described in detail in the chicken *Gallus gallus* (Woodson, Reiner, Anderson, & Karten, 1991), the quail *Coturnix japonica* (Uchiyama, Yamamoto, & Ito, 1996; Uchiyama & Watanabe, 1985), and the pigeon *Columbia livia* (Miceli, Repérant, Bavikati, Rio, & Volle, 1997, Miceli, Repérant, Marchand, & Rio, 1993; Woodson, Reiner, Anderson, & Karten, 1991). In addition to the proper ION, a smaller number of morphologically different "ectopic centrifugal neurons" lie in surrounding areas (Clarke & Cowan, 1975). Barely any data exist on their afferents (Repérant et al., 2006), though they might also receive tectal projections (O'Leary & Cowan, 1982; Woodson et al., 1991). The axons of both ION and ectopic centrifugal neurons project to the retina where they terminate at the border of the inner plexiform layer (IPL) and the inner nuclear layer (INL) (Chmielewski, Dorado, Quesada, Geniz-Galvez, & Prada, 1988; Dogiel, 1895; Hayes & Holden, 1983). The axons of the ION neurons form "convergent" terminals (Fritzsch, de Caprona, & Clarke, 1990; Uchiyama & Ito, 1993), which are dense pericellular nests on "association amacrine cells" (AACs) in the INL (Fischer & Stell, 1999; Lindstrom et al., 2009; Nickla et al., 1994; Ramón y Cajal, 1911, 1893; Uchiyama & Ito, 1993; Uchiyama & Stell, 2005). The AACs have axons and project to other parts of the retina (Catsicas, Catsicas, & Clarke, 1987a; Lindstrom, Azizi, Weller, & Wilson, 2010; Uchiyama, Aoki, Yonezawa, Arimura, & Ohno, 2004; Uchiyama & Barlow, 1994). Axons from ectopic centrifugal neurons, however, form "divergent" terminals, which broadly ramify in the IPL (Fritzsch et al., 1990; Woodson et al., 1995). Little is known about their postsynaptic targets, though it has been reported that they might contact displaced ganglion cells (Dogiel, 1895; Hayes & Holden, 1983; Maturana & Frenk, 1965; Nickla et al., 1994) and "flat" amacrine cells (Dogiel, 1895; Maturana & Frenk, 1965).

In contrast to Neognathae, birds of the order Palaeognathae which comprises Struthioniformes (ostriches), Rheiformes (rheas), Tinamiformes (tinamous), Apterygiformes (kiwis), and Casuariiformes (cassowary and emu; Prum et al., 2015), seem to lack a proper ION (Craigie, 1930; Gutiérrez-Ibáñez, Iwaniuk, Lisney, Faunes, Marín, & Wylie, 2012; Verhaart, 1971). Nonetheless, as we previously demonstrated by neural tracing in the Chilean Tinamou (*Nothoprocta perdicaria*), they do possess a high number of centrifugal visual neurons, which form a loosely congregated complex in the same isthmic region where an ION would be expected (Krabichler, Vega-Zuniga, Morales, Luksch, & Marín, 2015). This different organization may implicate structural and functional differences of the centrifugal visual system of Palaeognathae compared with Neognathae; however, the circuitry of palaeognathous centrifugal visual system in the brain and retina is still completely unknown (Figure 1b). Since Palaeognathae diverged from their sister clade Neognathae ~100 million years ago (see Figure 2; Brusatte,

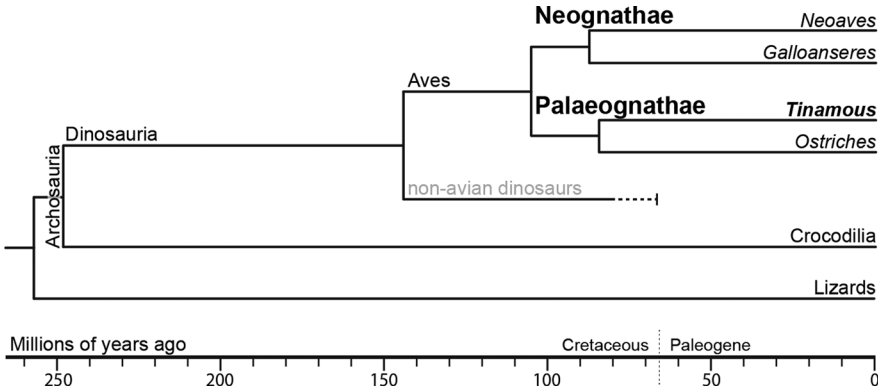

FIGURE 2 Abbreviated cladogram showing the position of Tinamous within the phylogenetic tree of the Archosauria. Phylogeny and divergence times are shown as inferred from a combination of nuclear and mitochondrial genome data and fossil markers (based on Brusatte et al., 2015, and Yonezawa et al., 2017). Note that the two grand extant clades of birds, Palaeognathae and Neognathae, are separated by ~100 million years of divergent evolution

O'Connor, & Jarvis, 2015; Claramunt & Cracraft, 2015; Jarvis et al., 2014), the comparative study of their differently organized centrifugal visual system may provide important insights into the evolution and behavioral significance of the avian centrifugal visual system, questions which continue to be unresolved in spite of many hypotheses put forward (e.g., Dillingham, Guggenheim, & Erichsen, 2013, 2017; Gutiérrez-Ibáñez et al., 2012; Marín, Letelier, & Wallman, 1990; Uchiyama, Ohno, & Kodama, 2012; Wilson & Lindstrom, 2011).

In the present study, we have combined in vivo and in vitro pathway tracing in the Chilean Tinamou, in order to reveal the principal elements and connectivity of the centrifugal visual system of a palaeognathous bird. We examine the morphology and neuroanatomy of the centrifugal neurons, their afferents from the TeO, the tecto-isthmo-optic neurons in the TeO, and the centrifugal terminals in the retina. We then compare these results with the well-studied neognathous centrifugal visual system and discuss possible implications for understanding the evolution and function of the avian centrifugal visual system.

2 | MATERIALS AND METHODS

Twenty-three adult Chilean Tinamous (*Nothoprocta perdicaria*) of both sexes (weight 398 ± 23 g [mean ± SD]), obtained from a Chilean breeder (Tinamou Chile, Los Ángeles, Chile) were used in this study. The animals were kept in the animals facilities of the Department of Biology at the Universidad de Chile, with food and water *ad libitum*. All efforts were made to minimize animal suffering, and the experiments were conducted in compliance with the guidelines of the NIH on the use of animals in experimental research, as well as with the approval of the bioethics committee of the Faculty of Sciences of the Universidad de Chile. For in vivo experiments, general anesthesia was induced by IM injection of a mixture of 40 mg/kg Ketamine (Ketamil, Troy Laboratories Pty Ltd, Glendenning, Australia; maximum total dose 120 mg/kg) and 2.5 mg/kg Xylazine (Xylavet, Alfasan International BV, Woerden, Holland; maximum total dose 7.5 mg/kg) and the bird was placed in a stereotaxic device immobilizing its head with ear bars and a beak holder. Body temperature was monitored via a cloacal thermometer and stabilized at 39–40°C by a heating pad connected to a feedback temperature control unit (Frederick Haer and Co., Brunswick, Maine, USA). Deep anesthesia during the experiments was maintained by 1–2% vaporized isoflurane delivered via a custom-built face mask at a constant flow of 200 ml/min oxygen, using a semiopen nonrebreathing Jackson-Rees circuit coupled to a gas anesthesia system (Matrx VIP 3000, Midmark, Dayton, OH).

2.1 | In vivo tracer injections

Three birds received intraocular injections of Cholera Toxin B subunit (CTB; #104, List Biological Laboratories Inc., Campbell, CA, USA). The skin covering the dorsal-most sclera of the closed eye was disinfected with 70% ethanol and diluted iodine. A Hamilton syringe (Reno, NV) with a sterile 30G cannula and loaded with 1% CTB in 0.1M phosphate buffered saline pH 7.4 (PBS; 0.75% NaCl) and 2% dimethyl sulfoxide (DMSO) was positioned using a micromanipulator. Skin and sclera were punctured and the further path of the cannula into the eye was ophthalmoscopically monitored. CTB (15 μl) were injected into the eye's vitreous body near the retina. After 10 min, the syringe was slowly retracted.

For the experiments with intracerebral injections of neuronal tracers, each bird first received an intraocular injection of 20 μl Rhodamine B isothiocyanate (RITC; Sigma-Aldrich Chemie GmbH, Steinheim, Germany; 10% in PB with 2% DMSO) into the eye contralateral to the experiment, analogous to the CTB injections, in order to retrogradely label the centrifugal visual neurons. Then, the head plumage was trimmed where necessary and the scalp was disinfected with 70% ethanol and diluted iodine. After exposing the skull by a longitudinal incision, craniotomy was performed to open a window overlying either the right TeO or the right telencephalic hemisphere. In the first set of experiments (n = 4), tracer was injected into the TeO. After exposing the tectal dura, a micropipette containing the neuronal tracer solution

was positioned perpendicular to the surface of the accessible TeO and inserted to depths between 600 and 800 μm. Either *Phaseolus vulgaris* leucoagglutinin (PHAL; Vector Laboratories Inc., Burlingame, CA, USA; 2.5% in PBS) or biotinylated dextran amine of 3 kDa (BDA, Thermo Fisher Scientific, Waltham, MA, USA; 10% in 0.1M phosphate buffer pH 7.4 [PB]) served as tracers. The PHAL injections were performed with an air-pressure system (Picospritzer II, General Valve, Fairfield, NJ) combined with iontophoresis (5 μA, 7s on/off pulse series, 10 min) using a Midgard Precision Current Source (Stoelting Co., Wood Dale, IL, USA). BDA was injected at volumes between 115 and 230 nl with a Nanoliter 2000 injector (World Precision Instruments, USA).

Another set of experiments (n = 12) aimed at injecting into the Tinamou's isthmo-optic complex (IOC). The heads of the birds were immobilized at a custom angle, in which the ear bars were in horizontal alignment with the beak commissure. In order to avoid cerebellar blood vessels, the IOC region was approached via the telencephalon, while the interhemispheric superior sagittal sinus (midline) served as orientation reference in the mediolateral dimension, and the transverse sinus of the cerebrocerebellar fissure in the anteroposterior dimension. After determining depth landmarks (such as the ventrocaudal telencephalic dura) by electrophysiological recordings with tungsten electrodes, a glass micropipette (tip diameter 30 μm) filled with CTB (1% in 0.1M PBS) was lowered to the stereotaxic coordinates of the IOC. Injections were performed with the Picospritzer combined with iontophoresis analogous to PHAL (see above). About 10 min after the injection in both sets of intracerebral experiments, the micropipette was slowly retracted, the craniotomy window was closed with the skull fragment and bone wax, and the skin wound was sutured.

After every experiment, sterile saline with an analgesic (Ketoprofen; Koralen 10%, Centrovet, Chile; 3 mg/kg) was administered SC and the animals were allowed to recover. After 5–10 days of survival, the birds were euthanized with an overdose of Ketamine/Xylazine IV and perfused through the arteriae carotides with 600 ml of warm saline followed by 300 ml of cold 4% paraformaldehyde (PFA) in PB. During the final minutes of the saline perfusion (before switching to PFA), the eyes were enucleated, hemisected at the ora serrata, freed from the vitreous body and fixed for 30 min in 4% PFA/PB. After PFA perfusion, the brain was dissected from the skull and postfixed in 4% PFA/PB overnight. Tissue was stored in PB containing 0.025% sodium azide. Brains and retinas were embedded in Gelatin (12% gelatin type A, 10% sucrose in H_2O at 37°C) and postfixed in 4% PFA/PB for 2 hr. After equilibration in a 30% sucrose/PB solution, tissue was cryosectioned on a sliding microtome at 45–60 μm.

2.2 | Retinal in vitro tracings

Four birds were euthanized by an overdose of Ketamine/Xylazine, their eyes immediately enucleated and hemisected, and the eye cups with the retinas (after removal of the vitreous with forceps) maintained in oxygenated (95% O_2/5% CO_2) Ames' Medium supplemented with 1.9 g/l sodium bicarbonate (AM; Sigma-Aldrich Chemie GmbH, Steinheim, Germany), at room temperature (RT). A Vaseline ring was formed around the severed optic nerve. After performing a fresh cut of the optic nerve stump, a drop of distilled water was applied on the stump for 5 min. Then, the water was removed and 2 μl of a solution of 10% Dextran, Alexa Fluor 546, 10,000 MW (Dextran10K-Alexa546; Thermo Fisher Scientific, Waltham, MA, USA) in H_2Od were pipetted onto the transected nerve. The site was covered with Vaseline and the preparation was transferred into fresh AM, where it was incubated for 12–18 hr under continuous oxygenation at RT, in the dark. Finally, the Vaseline was removed and the eye cup was rinsed in PB, followed by fixation in 4% PFA/PB for 30 min. Tissue was stored in PB containing 0.025% sodium azide. The retinas were extracted and whole mounted (Ullmann, Moore, Temple, Fernández-Juricic, & Collin, 2012), embedded in Gelatin (see above), and cryosectioned in the horizontal (flattened) plane at 60 μm.

2.3 | NADPH-diaphorase histochemistry

Nicotinamide adenine dinucleotide phosphate (NADPH)-diaphorase histochemistry was conducted following the method described in Fischer & Stell (1999). Briefly, slides carrying retinal sections were washed three times in 0.1 M Tris-Buffer (pH 8.0) and then incubated in 0.1 M Tris-buffer with 1 mg/ml β-NADPH (Sigma-Aldrich Chemie GmbH, Steinheim, Germany; Cat# N5130), 0.4 mg/ml nitrotetrazolium blue (Sigma-Aldrich Chemie GmbH, Steinheim, Germany; Cat# N6876), 2 mg/ml $CaCl_2$ and 0.3% Triton X-100, for 60 min at 37°C.

2.4 | Immunohistochemistry

All antibodies used in this study are listed in Table 1, including their specifications, RRID, and dilutions. For anti-CTB and anti-PHAL immunohistochemistry, sections were first immersed in 90% methanol/3% H_2O_2 for 12 min to quench endogenous peroxidase activity. After rinsing in PBS, they were incubated overnight at RT in a solution with primary antibodies goat anti-CTB (RRID:AB_10013220) or goat anti-PHAL (RRID:AB_2315144) diluted in PBS/Triton X-100 (PBS-Tx) 0.3% with 5% normal rabbit serum, followed by rinsing in PBS and incubation with a secondary antibody (biotinylated rabbit anti-Goat [RRID: AB_2336126] diluted in PBS-Tx 0.3% for 2 hr at RT). After rinsing, avidin-biotin peroxidase complex (ABC; Vectastain Elite ABC Kit, Vector Laboratories Inc., Burlingame, CA, USA; 3.2 μl/ml in PBS-Tx 0.5%/4% NaCl) was added. Finally, detection was accomplished by diaminobenzidine (DAB) precipitation in a solution of 0.025% DAB (DAB-buffer tablets for microscopy, Merck KGaA, Darmstadt, Germany), 0.0025% H_2O_2, 0.069% imidazole and 1% $NiSO_4$ in 0.175M acetate buffer, pH 6.0 (Green, Sviland, Malcolm, & Pearson, 1989). For fluorescence microscopy, sections were incubated for 2 hr with Streptavidin-Alexa488 (Streptavidin Alexa Fluor® 488 conjugate, Thermo Fisher Scientific, Waltham, MA, USA) diluted 1:600 in PBS-Tx 0.5%. In cases where BDA was used as a tracer, ABC/DAB or Streptavidin-Alexa488 was applied as above, but directly after the quenching step without primary/secondary antibodies. Retinal sections were reacted for immunofluorescence against Parvalbumin. Tissue was blocked in PBS-Tx 0.5% with 1% bovine serum albumin and 10% normal goat serum. It was incubated over night at RT in primary antibody mouse anti-Parvalbumin (RRID:AB_477329), diluted in PBS-Tx 0.5%. After 4x

TABLE 1 Antibodies used in this study.

Antibody	Antigen	Immunogen	Source, Cat. #, Host species, clonality, RRID	Dilution
anti-CTB	CTB (cholera toxin B subunit)	Purified choleragenoid (cholera toxin B subunit aggregate)	List Biological Laboratories Inc., Campbell, CA, USA; Cat# 703; Lot. 7031E; goat (polyclonal) RRID:AB_10013220	1: 40,000
anti-PHAL (biotinylated)	PHAL (*Phaseolus vulgaris* leucoagglutinin)	Purified *Phaseolus vulgaris* erythro/leucoagglutinin (E+L)	Vector Laboratories Inc., Burlingame, CA, USA; Cat# BA-0224; Lot. W1121; goat (polyclonal) RRID:AB_2315144	1: 2,000
anti-Parvalbumin	Parvalbumin	Purified frog muscle parvalbumin	Sigma-Aldrich Chemie GmbH, Steinheim, Germany; Cat# P3088; Lot. 122M4774V; mouse (monoclonal) RRID:AB_477329	1: 2,000
biotinylated anti-Goat, made in rabbit	Goat IgG (H+L)	Purified goat IgG	Vector Laboratories Inc., Burlingame, CA, USA; Cat# BA-5000; rabbit RRID:AB_2336126	1: 1,500
Alexa Fluor 488 anti-Mouse, made in goat	mouse IgG (H+L)	mouse IgG (H+L)	Thermo Fisher Scientific, Rockford, IL, USA; Cat# A-11029; Lot. 1170049; goat (polyclonal) RRID:AB_2534088	1: 500

rinsing in PBS, secondary antibody Alexa Flour 488 goat anti-Mouse (RRID:AB_2534088; diluted in PBS-Tx 0.1%) was added for 6 hr at RT. The mouse anti-Parvalbumin generated against purified frog muscle Parvalbumin is highly specific and recognizes a single band of ~12 kDa in Western blots of lysed brain tissue, the molecular weight of Parvalbumin (Ramamurthy & Krubitzer, 2016).

2.5 | Tyramide Signal Amplification

In the present study, some tracings of thin neural connections had originally produced falsely negative results. Despite the high sensitivity of our tracer of choice CTB (Angelucci, Clascá, & Sur, 1996) in these cases, standard protocols failed to reveal relevant neuroanatomical details. This indicates that thin or sparse neural circuits may have such low tracer uptake and transport that the sensitivity of standard immunohistochemistry is insufficient to detect them. We found that these limitations could be overcome by tyramide signal amplification (TSA). This method, applied after the ABC step, strongly amplifies the immunohistochemical signal. In the presence of H_2O_2, the peroxidase activity causes the formation of short-lived radicals of biotin-labeled tyramide, which covalently bind to any nucleophilic residues nearby (Bobrow, Harris, Shaughnessy, & Litt, 1989) and potentiate the biotin-sites available for further detection. Although TSA has been widely used in e.g., in situ hybridization techniques, it has very seldom been combined with neuronal tracing (Adams, 1992; Papp & Palkovits, 2014). Our results suggest that by revealing fine neuroanatomical details which would otherwise remain hidden, TSA has the potential to upgrade classical in vivo tracing experiments to satisfy the elevated demands of modern microconnectomics (Swanson & Lichtman, 2016; Vega-Zuniga et al., 2016). For performing TSA, protocols up to the ABC step were identical to above. Then, brain- and retina-sections were incubated in 0.0001% biotin-tyramide (IRIS Biotech GmbH, Marktredwitz, Germany; Cat# LS-3500, Lot. 1407008) and 0.003% H_2O_2 in 0.05M borate buffer, pH 8.5, for 30 min. After washing, final detection was performed with either a second ABC step followed by DAB, or Streptavidin-Alexa488 (see above).

2.6 | Analysis

Sections were mounted on gelatin-coated slides, counterstained according to standard Nissl or Giemsa protocols or left clear, and cover-slipped with DPX Mountant (Sigma-Aldrich Chemie GmbH, Steinheim, Germany; after dehydration/xylene clearing), or *n*-propyl gallate fluorescence mounting medium (Giloh & Sedat, 1982). Microscopy was performed with an Olympus BX63 microscope with attached digital cameras (DP26 color for brightfield, XM10 monochrome for epifluorescence), or an Olympus Fluoview FV1000/BX61 confocal laser scanning microscope (Olympus, Tokyo, Japan). Images were processed in the microscope software (Olympus Fluoview FV10-ASW v04.02.01.20, RRID:SCR_014215; or CellSens Dimension v1.7, RRID:SCR_014551) and the ImageJ distribution Fiji (Schindelin et al., 2012; RRID:SCR_002285).

3 | RESULTS

3.1 | Anatomy of the IOC

As previously reported (Gutiérrez-Ibáñez et al., 2012; Krabichler et al., 2015), the palaeognathous Chilean Tinamou appears to lack an ION in brain sections counter-stained with Nissl or Giemsa (Figure 3a,b). However, a CTB injection into the eye retrogradely labels a large number of centrifugal visual neurons in the contralateral isthmic region, as well as a smaller number on the ipsilateral side (Figure 3c; Krabichler et al., 2015). We suggest to call this cell group "isthmo-optic complex" in Palaeognathae, in order to distinguish it from the ION of neognathous birds. For the present study, we did several new intraocular tracing experiments with CTB and sectioned the brains in different planes (transverse and horizontal) in order to get a better picture of the IOC's neuroanatomy.

The isthmo-optic tract, which contains the centrifugal axons toward the retina, took the same trajectory as in neognathous birds (Galifret, Condé-Courtine, Repérant, & Servière, 1971), leaving the IOC dorsolaterally (Figure 4aa, b), then coursing rostrally along the dorsal rim of the TeO (Figure 4aa–ab; cf., figures 7f and 11b in Krabichler

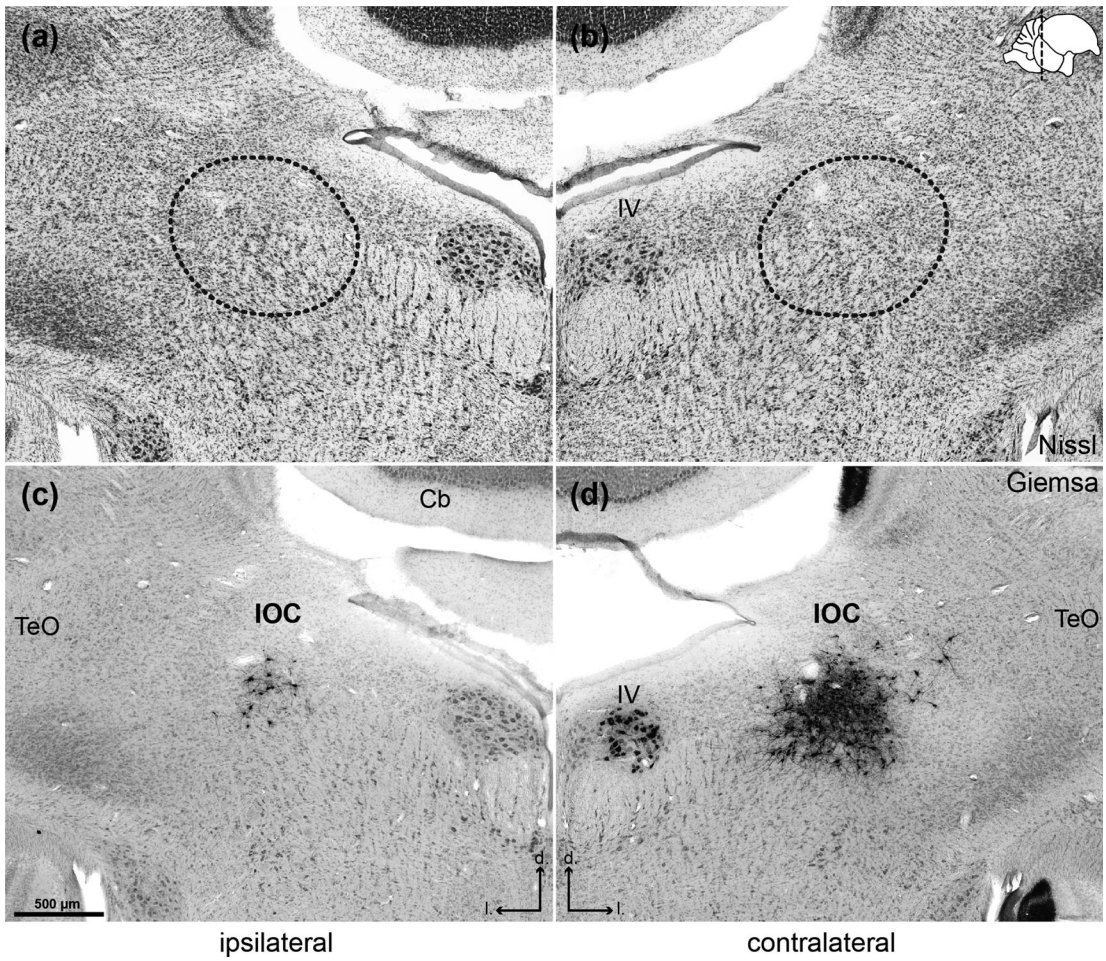

FIGURE 3 The isthmo-optic neurons in the Chilean Tinamou do not form a clear isthmo-optic nucleus (ION). (a and b) In Nissl-stained brain sections at the level of the isthmus, an ION is not distinguishable. (c and d) Adjacent sections from the same brain as in (a) and (b), but processed for immunohistochemical detection of intraocularly injected tracer Cholera Toxin B subunit (CTB) and counterstained with Giemsa. This reveals a diffuse but cell-rich cluster of retrogradely labeled IO neurons, the isthmo-optic complex (IOC). A large number of CTB-positive cells are found contralateral to the injected eye (d), while few are marked on the ipsilateral side (c).Orientation: *d*. dorsal; *l*. lateral. Abbreviations: TeO, optic tectum; Cb, cerebellum; IV, trochlear nucleus. Adapted from "The visual system of a Palaeognathous bird: Visual field, retinal topography and retino-central connections in the Chilean Tinamou (*Nothoprocta perdicaria*)" by Krabichler et al., 2015, Journal of Comparative Neurology, 523, 226–250

et al., 2015) and finally joining the rostroventral stratum opticum in direction of the optic nerve. The IOC was found in a topologically similar position as the neognathous ION (Figure 4aa–ad). It was located dorsally in the isthmic region and measured ~600–700 μm mediolaterally, 700 μm anteroposteriorly and 800–900 μm dorsoventrally. On its lateral side, it was bordered by the dorsal nucleus of the lateral lemniscus (LLD) and the formatio reticularis lateralis (FRL). Ventral to it lay the A8 dopaminergic cell group (formerly known as rostral locus coeruleus; Reiner et al., 2004), as indicated by a dense cluster of anti-tyrosine-hydroxylase-positive neurons in this region (data not shown). Dorsally and dorsomedially, the IOC was separated from the tegmental pia by a cell-rich region, which according to its cytoarchitecture might be part of the central gray.

In contrast to the ION of most Neognathae, which is a clearly demarcated, laminarly organized nucleus, the Tinamou's IOC was less well-structured. Nevertheless, most retinopetal (CTB-positive) neurons were located in a densely packed "core" region (Figure 4b,c,e), while a smaller number of "ectopic" cells was found further away at distances of as much as 500 μm or more (see arrows in Figure 4b,c). The ipsilaterally projecting neurons also mostly lay within the IOC core, and no bilaterally projecting IOC neurons were found after injecting different types of fluorescent CTB (CTB Alexa 488 and 546) into the eyes. Despite its density, the boundary of the IOC core region was not clearly circumscribed but merged into the surrounding neuronal areas. Apart from centrifugal (CTB-positive) neurons, the IOC also contained Nissl-stained CTB-negative neurons (Figure 4d), which might either be interneurons or cells from different structures lying interspersed with the IOC neurons.

All CTB-positive IOC neurons had a multipolar morphology with numerous primary dendrites splitting off in various directions (Figure 4e, f). Within the IOC core, the neurons were embedded in a dense neuropil from their dendrites (Figure 4e, f). They showed no sign of laminar

orientation or any other kind of regular organization, as can be seen in both the transverse (Figure 4b) and the horizontal plane (Figure 4c,e). The diffuse boundary of the IOC core was indicated by a notable decrease in density of the neuropil (Figure 4e). Interestingly, beyond the core region a number of dendrites extended radially away and deep into surrounding tissue (arrowheads in Figure 4b,c). While some of them may have belonged to peripheral IOC neurons, many could indeed be observed to originate from neurons within the core (see arrowheads in Figure 4e for a clear example). They were particularly numerous and long toward ventral, rostral, and medial, where they reached into adjacent neural structures such as A8, while sparing more lateral structures such as the LLD (Figure 4aa–ac,b).

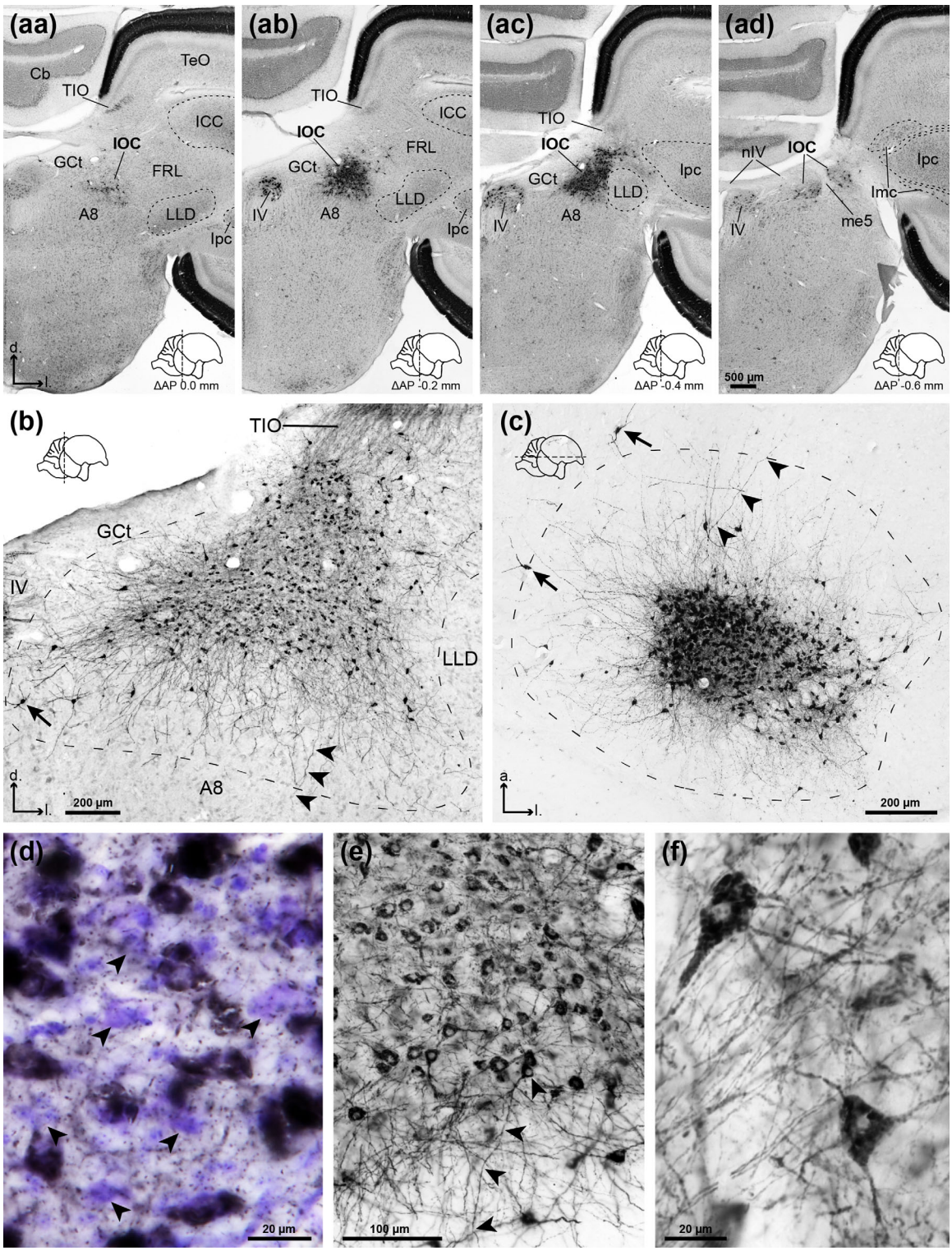

FIGURE 4.

3.2 | The tectal afferents to the IOC

Prompted by the unusual appearance of the IOC, we examined its afferents. In Neognathae, the strongest projection to the ION arises from neurons in L9-10 of the TeO (Cowan, 1970; Uchiyama et al., 1996; Woodson et al., 1991). Therefore, we injected PHAL (n = 2) and BDA (n = 2) into the TeO of the Chilean Tinamou in order to anterogradely label the tectal afferents to the IOC, and RITC (red fluorescence) into the contralateral eye to retrogradely label the retinopetal IOC neurons. Like CTB, RITC reliably labeled the complete extent of retinal projections to the TeO (Figure 5a) as well as all retinopetal IOC neurons.

In all cases, the injection sites in the TeO were well-defined and lay predominantly centered in the intermediate tectal layers (L8–12). A representative case of an injection with BDA is shown in Figure 5. The injection site extended from L9 to L13 with no tracer spill or diffusion into other parts (Figure 5a,b). The nucleus isthmi pars parvocellularis (Ipc), which characteristically receives a topographic projection from L10 of the TeO, contained a confined band of labeled tectal fibers and retrogradelly labeled neurons. In all cases, BDA-labeled axons were present ventral to the inferior colliculus (IC; in birds also known as MLd, nucleus mesencephalicus lateralis pars dorsalis) and dorsal to the Ipc (Figure 5c), that is, in an equivalent position as the tecto-isthmal tract to the ION in Neognathae. While some of these fibers (see arrows in Figure 5c) bent ventrally toward the Ipc, others (see arrowheads in Figure 5c) could clearly be traced medially toward the IOC.

Tecto-IOC fibers were consistently found terminating in the IOC core region amidst the retrogradely labeled retinopetal neurons (Figure 5d–g). The terminals tended to branch (see arrows in Figure 5d,f) and diverge into delicate fields which sometimes spanned considerable areas (Figure 5f). Distal ramifications of the terminals contained many varicosities (Figure 5g), while fewer were also present on short side branches or "*en passant*" (see arrowheads in Figure 5d–f). Often, varicosities were found in immediate proximity to somata (see lower arrowheads in Figure 5e,g) or dendrites (see upper arrowheads in Figure 5g) of RITC-labeled cells, suggesting a monosynaptic projection from the TeO to the centrifugal IOC neurons. In other cases, varicosities were found without any immediate RITC-labeled target structure nearby (see e.g., upper arrowheads in Figure 5e). These may have either contacted more distal dendrites of centrifugal IOC neurons that were not well labeled by RITC (even compared with CTB; cf. Figure 4e,f), or interneurons (cf. Figure 4d). In the areas surrounding the IOC core, no tecto-IOC terminals were found in spite of the numerous radial IOC dendrites which traverse these regions (see above; Figure 4b,c).

These results show that the TeO in the Chilean Tinamou gives rise to a projection to the IOC core region, where widespread varicose ramifications form "divergent" terminals. As the injection sites were in all cases centered in the intermediate tectal layers, the cells-of-origin of the tecto-IOC projection were likely to be found there. Next, we did in vivo injections into the IOC in order to retrogradely label and identify these "tecto-IOC" neurons.

3.3 | The tecto-IOC neurons

CTB was injected into the isthmic region of 12 Chilean Tinamous, while contralateral intraocular RITC injections again served to reveal the IOC. In five cases, the injection site covered the IOC, while the remaining unsuccessful injections served as controls. Figure 6 shows sections from one representative case of a successful injection, amplified with TSA (see Methods). Although in this case the injection site was not completely centered in the IOC (Figure 6a), the existence of many CTB/RITC-double-labeled IO neurons (Figure 6b) demonstrated that a substantial portion of the IOC was covered by the CTB injection.

In the TeO of all successful IOC injections, retrogradely labeled neurons were found in L10, while other layers (except the deep layers L13-15; see Discussion) were devoid of labeled cells. Specifically, these presumptive tecto-IOC neurons lay in the more superficial portion of

FIGURE 4 Detailed anatomy of the Chilean Tinamou's isthmo-optic complex (IOC) labeled by intraocular injection of Cholera Toxin B subunit (CTB). (aa–ad) Antero-posterior series of coronal sections showing the neuroanatomical location and dimension of the IOC in the dorsal isthmus. It is found at the level of the trochlear nucleus (IV) and trochlear nerve (nIV), and is surrounded by the dorsal nucleus of the lateral lemniscus (LLD), formatio reticularis lateralis (FRL), central gray (GCt), and field A8. In the TeO, anterogradely labeled retinal projections are also CTB-positive (dark staining). Section planes with relative stereotaxic coordinates are indicated by the schemata at the bottom. (b) A coronal section through the IOC. The isthmo-optic tract (TIO) can be seen leaving the IOC dorsally. The IOC contains a core region densely packed with IO neurons and their dendrites. Some peripheral IO neurons are located relatively far away from the IOC core (arrow). Dendrites originating from the core region can be found extending away into surrounding neural structures, such as A8 (arrowheads). (c) A horizontal section through the IOC, showing the dense core region and few single IO neurons (arrows) lying at considerable distances from it. The radially extending core dendrites (arrowheads) are predominantly directed toward anterior and medial. (d) High power photomicrograph within the IOC core in a section counterstained with Nissl. Among the CTB-positive IO neurons (dark DAB-staining), many CTB-negative neurons (arrowheads) can be found, which might be interneurons. (e) Medium power photomicrograph of the IOC core region with its numerous multipolar IO neurons. Within the core, the dendritic neuropil has a very high density (see also f), which however rapidly declines at the border of the core region *(bottom)*. Some core neuron dendrites extend beyond the border (arrowheads), indicating that the IOC's radially extending dendrites (cf. b and c) may largely originate from within the core. (f) High power photomicrograph of two IOC neurons in the IOC core. Note their multipolar morphology and the dense dendritic neuropil that surrounds them. Orientation: *a*. anterior; *d*. dorsal; *l*. lateral. Abbreviations: *A8* field A8; *Cb*, cerebellum; *FRL*, formatio reticularis lateralis; *GCt*, central gray; *ICC*, central subnucleus of the inferior colliculus (in birds also known as nucleus mesencephalicus lateralis pars dorsalis, MLd); *Imc*, nucleus isthmi, pars magnocellularis; *Ipc*, n. isthmi, pars parvocellularis; *LLD*, dorsal n. of the lateral lemniscus; *me5*, mesencephalic trigeminal tract; *IV*, trochlear nucleus; *nIV*, trochlear nerve; *TeO*, optic tectum; *TIO*, isthmo-optic tract [Color figure can be viewed at wileyonlinelibrary.com]

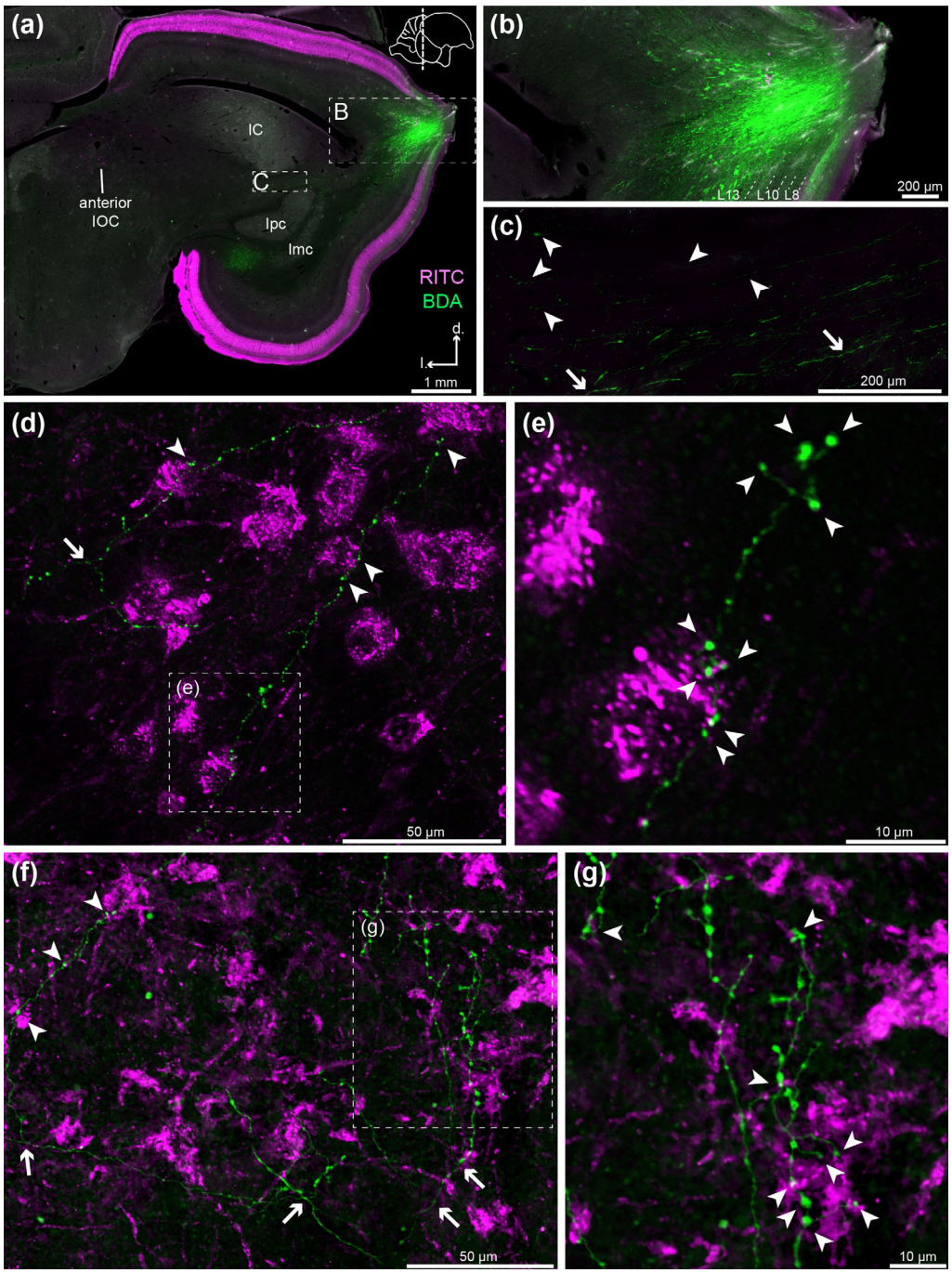

FIGURE 5 Tecto-IOC terminals after tracer injections into the TeO. Confocal microscopy images in transverse brain sections (section plane indicated by pictogram in upper right corner in a). *Magenta*: tracing after intraocular injection of Rhodamine B isothiocyanate (RITC). *Green*: Biotinylated dextran amine 3 kDa (BDA) injected into the TeO, revealed by Streptavidin-Alexa488. (a) Low-power photomicrograph of a coronal section containing the BDA-injection site in the TeO (green). The retinal projections to the TeO as well as the anterior portion of the IOC are labeled by RITC (magenta). (b) High-power photomicrograph of the tectal injection site, which was centered in the intermediate layers (L8–12). (c) BDA-labeled axons in the region of the tecto-isthmal tract between IC and Ipc (see inset in *a*). While some axons bend toward the isthmi nuclei Ipc and Imc (arrows), others run in direction of the IOC (see arrowheads). (d) BDA-labeled tecto-IOC terminals, which ramify (see arrow) among the IOC neurons, have a varicose appearance, and some varicosities are found in close proximity to IOC neurons (arrowheads). (e) Enlargement of inset in *d*. Varicosities can be found in immediate opposition to an IOC neuron soma (bottom arrowheads) as well as at some distance (top arrowheads). Short side-branches can be distinguished in both cases. (f) "Divergent" tecto-IOC terminal which splits into wide ramifications (arrows). (g) Enlargement of inset in *f*. Many varicosities of a terminal arborization lie in direct proximity to RITC-labeled IOC somata or dendrites (arrowheads), indicating synaptic contacts. Orientation: *d*. dorsal; *l*. lateral. Abbreviations: *IC*, inferior colliculus (in birds also known as nucleus mesencephalicus lateralis pars dorsalis, MLd); *Imc*, nucleus isthmi, pars magnocellularis; *Ipc*, n. isthmi, pars parvocellularis [Color figure can be viewed at wileyonlinelibrary.com]

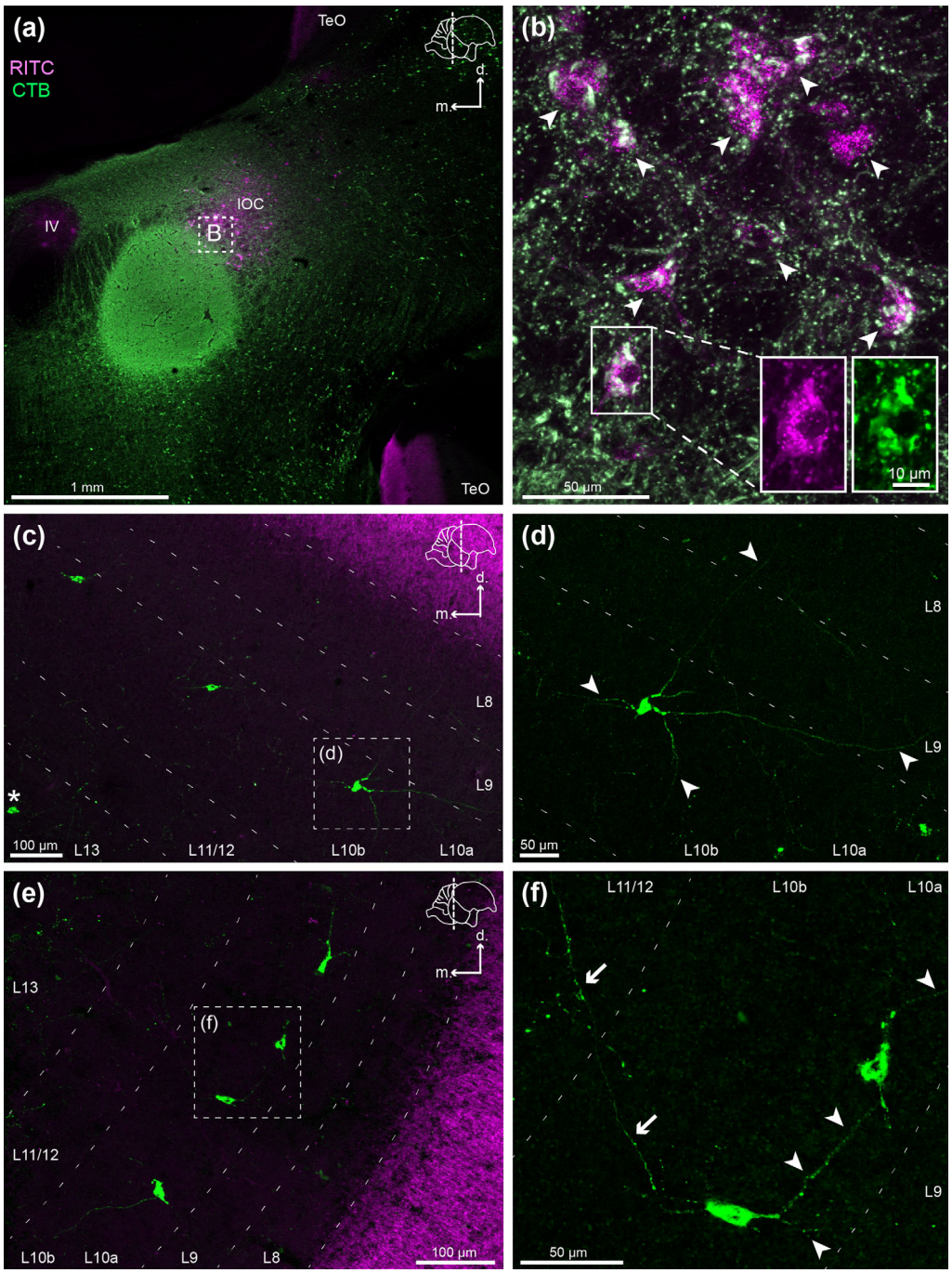

FIGURE 6 Tecto-IOC projection neurons in the TeO, retrogradely labeled by tracer injections into the IOC region. Confocal microscopy images of a representative case in which the injection partly covered the IOC. Transverse brain sections (section plane indicated by pictograms in upper right corners). *Magenta*: intraocularly injected Rhodamine B isothiocyanate (RITC). *Green*: Cholera Toxin B subunit (CTB) revealed by immunofluorescence (intensified by TSA; see Methods). (a) Injection site in the IOC region. (b) High-power photomicrograph of position indicated by inset in a. Although the center of the CTB injection only partly covered the IOC, many centrifugal visual neurons in the middle of the IOC were double-labeled with RITC and CTB (see arrowheads), indicating that the injection sufficiently spread into the IOC zones. (c–f) Presumptive tecto-IOC neurons in layer (L) 10a of the TeO retrogradely labeled by CTB, found in regularly spaced groups at various tectal positions. (c) Group of tecto-IOC neurons in the rostrodorsal TeO. An asterisk indicates a labeled neuron in L13, which probably belongs to a descending tectal projection that passes through the area of the injection. (d) High-power photomicrograph of one tecto-IOC neurons (see inset in *c*), showing its multipolar dendritic morphology (see arrowheads) (e) Group of tecto-IOC neurons in the caudoventral TeO, apparently with a narrower interneuronal spacing. (f) High-power photomicrograph of one of them (see inset in *e*). Some dendrites extend across the inter-neuronal space toward neighboring cells while others extend more radially through the TeO (see arrowheads). The axon which projects upon the IOC, splits off some collateral branches which terminate in L11/12 (see arrows) [Color figure can be viewed at wileyonlinelibrary.com]

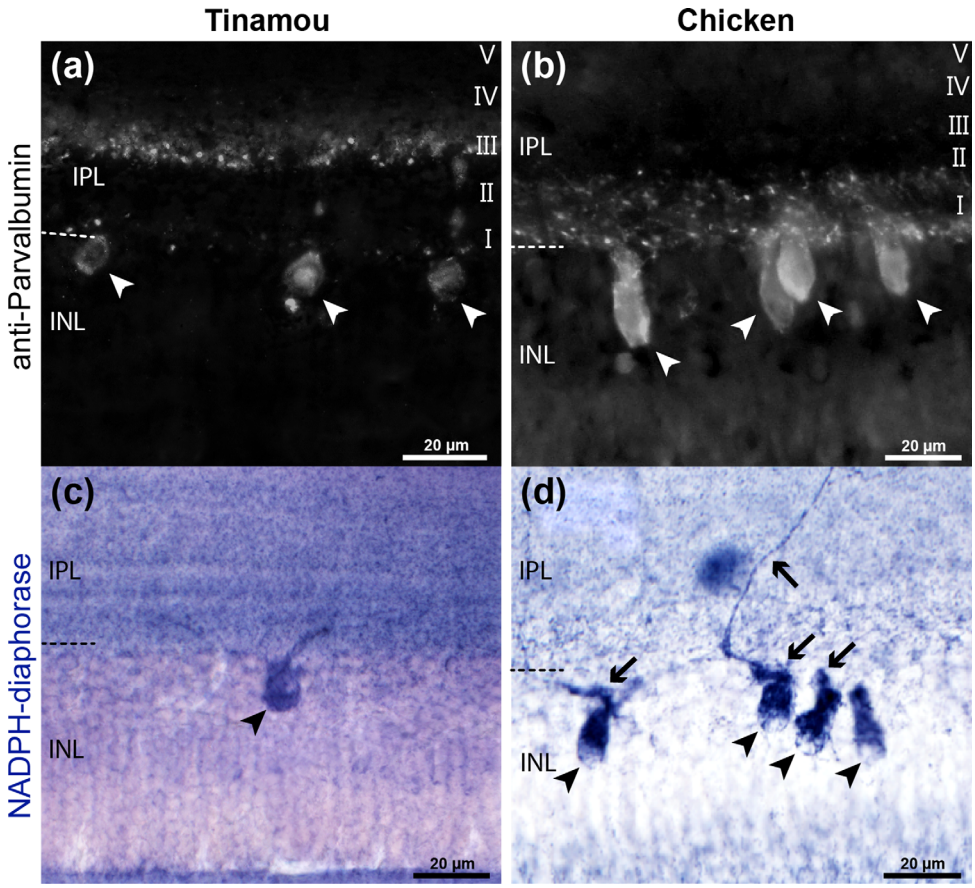

FIGURE 7 Histochemical comparison of centrifugal visual system elements in transverse sections of the retina of the Chilean Tinamou and the domestic chicken. (a and b) Anti-Parvalbumin immunofluorescence in the Tinamou (a) and the chicken (b). Labeled cell types are found in in the inner nuclear layer (INL) of both species (arrowheads). However, the Tinamou does not appear to possess cells which resemble the conspicuous elongated "association amacrine cells" (AACs) easily identified in the chicken (see arrowheads in b). (Note that the thickness of IPL sublamina I in b appears overrepresented due to the collapsed z-stack image.) (c and d) NADPH-diaphorase histochemistry in the Tinamou (c) and the chicken (d). In the chicken, this again labels the elongated AACs (see arrowhead in d) and also the "convergent" terminals (see arrows in d) from centrifugal ION fibers in the IPL, which synapse on AACs. In the Tinamou, although NADPH-diaphorase-positive cell types are present (see arrowhead in *c* for an example), none can be identified as AACs by any given criteria. Furthermore, no NADPH-diaphorase-positive "convergent" centrifugal visual terminals are found [Color figure can be viewed at wileyonlinelibrary.com]

L10, designated as L10a (Figure 6c,e). They were generally not very numerous, but in some parts of the TeO groups of them occurred together and formed a sparse, regularly spaced monolayer (Figure 6c,e). The interneuronal spacing varied from ~100–150 μm in the caudoventral TeO (Figure 6e) to ~300 μm in the rostrodorsal TeO (Figure 6c). The presumptive tecto-IOC neurons had oval-shaped somata and appeared to be multipolar (Figure 6d) possessing both obliquely horizontal and radially ascending/descending dendrites. Although some had an almost bipolar appearance (Figure 6c,f), they assumedly possessed additional dendrites not labeled by CTB. In cases where the dendrites were sufficiently labeled by CTB, they could be traced to ascend up to at least L8 and descend down to L10b (Figure 6d). Horizontal and obliquely horizontal dendrites extended across the intercell spacing toward the neighboring tecto-IOC neurons (see arrowheads in Figure 6f). In cases in which the axons were labeled, they were found to descend from the soma through the deep tectal layers (see arrows in Figure 6f), splitting off some thin collateral terminals with varicosities in L11-12 (see upper arrow in Figure 6f). Importantly, in the control cases where the injection site did not cover any part of the IOC but only nearby surrounding structures, no labeled neurons were found in L10 nor in other intermediate tectal layers. Only the deep layers (L13–15) also contained labeled neurons, which represented tectal pathways to (or passing through) areas surrounding the IOC (see Discussion).

3.4 | The centrifugal visual projection to the retina

In Neognathae, the main retinal target cells of the ION, the "association amacrine cells", are known to be positive for Parvalbumin (Fischer & Stell, 1999; Lindstrom et al., 2009; Sanna et al., 1992; Uchiyama & Stell, 2005) as well as NADPH-diaphorase, while the latter is additionally present in the prominent "convergent" centrifugal terminals (Fischer & Stell, 1999; Lindstrom et al., 2009; Morgan, Miethke, & Li, 1994; Nickla et al., 1994). In order to analyze whether these markers also reveal the retinal components of the palaeognathous centrifugal

visual system, we performed anti-Parvalbumin immunohistochemistry and NADPH-diaphorase histochemistry in transverse sections of the Chilean Tinamou retina. The chicken (*Gallus gallus*) served as a neognathous control.

In the Tinamou retina, various Parvalbumin-positive INL cell types were found, of which representatives are shown in Figure 7a. Their labeled processes stratified in IPL sublamina III, where they formed a clearly labeled band. None of the labeled cells in the Tinamou resembled the intensely Parvalbumin-positive AACs found in the ventral retina of the chicken (Figure 7b), which had the characteristic elongated morphology (Fischer & Stell, 1999; Lindstrom et al., 2009) and neurite stratification in IPL sublamina I (Fischer & Stell, 1999; Sanna et al., 1992). Analogous to these findings, NADPH-diaphorase histochemistry labeled various INL cell types in the Tinamou (see Figure 7c for an example), but none comparable to the elongated NADPH-diaphorase-positive AACs of the chicken (see arrowheads in Figure 7d). The latter were furthermore directly contacted by intensely NADPH-diaphorase-positive "convergent" centrifugal terminals (see arrows in Figure 7d), while in the Tinamou's retina no convergent NADPH-diaphorase-positive centrifugal fibers or terminals were observed.

Two different approaches were employed to label the centrifugal fibers in the Tinamou retina: First, we performed in vitro tracings with Dextran10K-Alexa546 from the optic nerve head of freshly dissected eye cups (see Methods), which were analyzed by confocal microscopy of horizontal (flatmount) retinal sections (Figure 8). The ganglion cell layer was strongly retrogradely labeled in many parts of the retina. In equatorial and ventral parts of the retina, the outer IPL (sublamina I) and border of the INL contained anterogradely labeled fibers with varicosities (Figure 8a). These presumptive centrifugal visual terminals were exclusively of the "divergent" type, forming a mesh of widespread horizontal ramifications (see filled arrowheads in Figure 8a). Their location at the IPL-INL border was corroborated by the presence of Parvalbumin-positive amacrine cells in the INL (see empty arrowheads in Figure 8b,c). The tracing also revealed retrogradely labeled displaced ganglion cells in the INL (see arrow in Figure 8a,c). Their dendrites also stratified in the IPL but had a smooth appearance which clearly distinguished them from the varicose centrifugal terminals (Figure 8a). The centrifugal terminals and displaced ganglion cell dendrites were mostly located in different strata. This can be seen in Figure 8d, which shows a reconstructed transverse section through the confocal z-stack volume, revealing two horizontal bands of Alexa-546 fluorescence signal. One band lay in sublamina II of the IPL and was primarily formed by displaced ganglion cell dendrites, which descended from the soma and

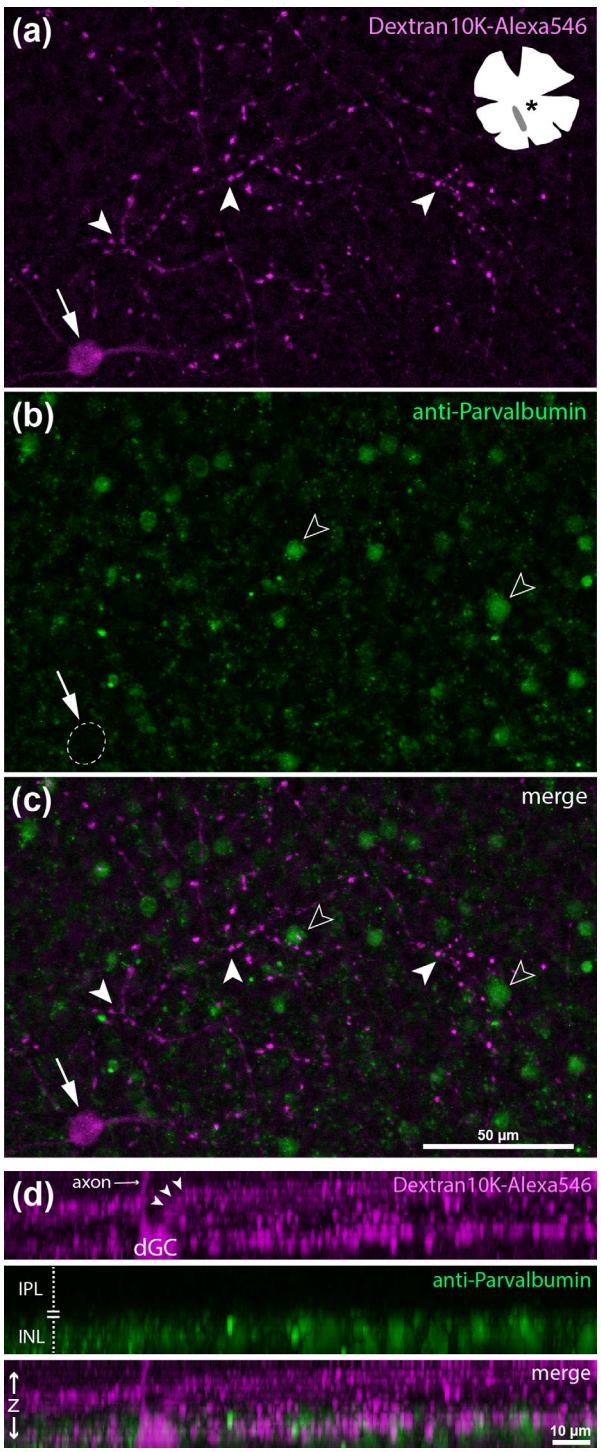

FIGURE 8 Centrifugal visual fibers and terminals in the Chilean Tinamou retina, labeled by in vitro tracing with Dextran10K-Alexa546. (a–c) Confocal photomicrograph in a horizontal retinal section at the level of the border between INL and IPL. Magenta corresponds to Dextran10K-Alexa546 (a), green to anti-Parvalbumin-immunofluorescence (b), and (c) shows the merge of both. Anterogradely labeled centrifugal terminals with many varicosities (magenta) can clearly be distinguished in the IPL. They lie in direct proximity to the INL marked by anti-Parvalbumin-labeled amacrine cells (green; see empty arrowheads). The terminals frequently ramify (see filled arrowheads) and form a big field. A retrogradely labeled displaced ganglion cell (dGC) is also present in the INL (note the smooth appearance of its dendrites). (d) Reconstruction of the *z* axis profile through the same confocal z-stack volume. The bulk of varicosity-rich centrifugal fibers (magenta) form a stratum in direct proximity to the INL. The INL can easily be identified by Parvalbumin-positive amacrine cells and a retrogradely labeled displaced ganglion cell whose axon ascends through the IPL. A second Dextran10K-Alexa546-labeled stratum is found where the dendrites of the displaced ganglion cell horizontally ramify [Color figure can be viewed at wileyonlinelibrary.com]

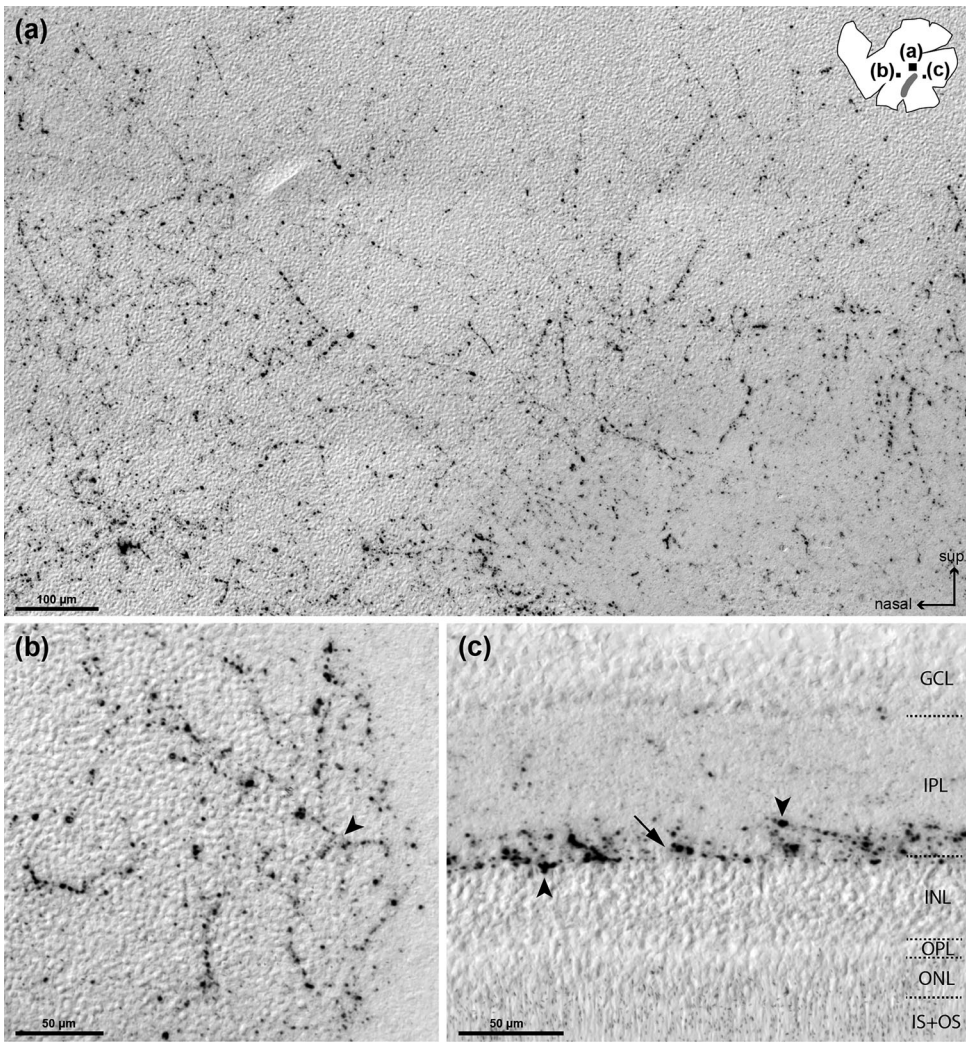

FIGURE 9 Centrifugal visual fibers and terminals in the Chilean Tinamou retina, labeled by in vivo tracing from the IOC. CTB-immunohistochemistry in the retina (TSA-enhanced; see Methods) after in vivo CTB-injections into the IOC (cf. Figure 5). The small pictogram in the upper right corner of A indicates the positions of the photomicrographs in the whole-mounted retina. (a and b) Horizontal sections of retinal whole-mounts. (a) Low-power differential interference contrast (DIC) photomicrograph at a central retinal position. A dense mesh of anterogradely labeled "divergent" centrifugal visual terminals is present in the retina at the border between IPL and INL (the cell-rich INL can be identified by the grainy appearance due to DIC). (b) Medium-power DIC photomicrograph at a nasal retinal position. An arriving centrifugal visual fiber terminal splits (see arrowhead) and ramifies into a varicosity-rich terminal. (c) High-power DIC photomicrograph of a transverse section through the retina. The centrifugal terminals (see arrowheads) mostly terminate around the border (see arrow) of INL and IPL, slightly protruding into the INL

stratified there (see arrowheads in Figure 8d; Wilson, Nacsa, Hart, Weller, & Vaney, 2011 Yang, Millar, & Morgan, 1989). Apart from those, only few varicosity-bearing fibers indicating centrifugal terminals were present here. The other more prominent band lay in IPL sublamina I at the border of (and protruding into) the INL, and (apart from a displaced ganglion cell soma) represented centrifugal terminals. In conclusion, the in vitro data suggest that most centrifugal terminals in the Tinamou lie in the IPL sublamina I adjacent to and protruding into the INL, while a minor portion might also terminate in IPL sublamina II.

Next, we processed the retinas of the in vivo IOC-injections for CTB-immunohistochemistry with TSA (see Methods), using again horizontal sections of retinal whole-mounts. Figure 9 shows differential interference contrast (DIC) photomicrographs from the contralateral retina of a representative case, which contained numerous centrifugal terminals of the divergent type. The majority of terminals were located in the equatorial and ventral retina. They formed a wide mesh of fibers (Figure 9a) and terminated in horizontal ramifications (Figure 9b). The granular surface of the INL can be distinguished to lie in the same focal plane as the centrifugal fibers and terminals. Transverse sections, produced in some parts of the retina due to tissue folds, confirmed that most centrifugal terminals lay at the border of IPL and INL (see arrow in Figure 9c), sometimes invading the INL (see lower arrowhead in Figure 9c), while a portion was present in sublamina I and presumably II of the IPL (see upper arrowhead in Figure 9c). Thus, our in vivo and in vitro data were in good agreement with each other. Furthermore, both

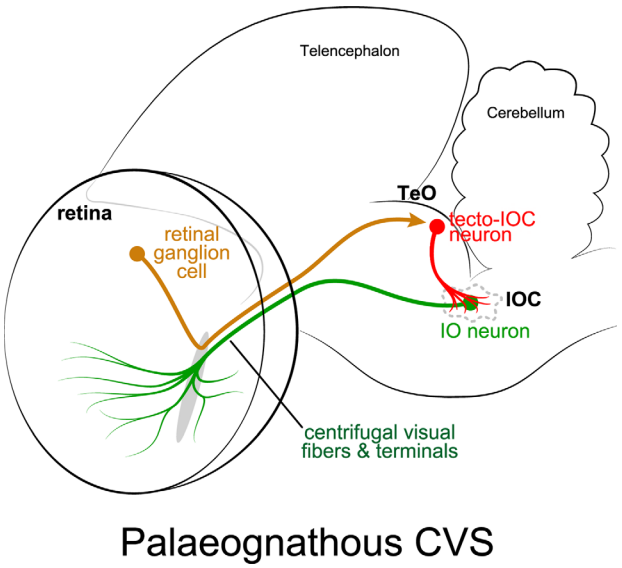

FIGURE 10 Schematic of the palaeognathous centrifugal visual system circuitry, updated by the new data. As shown by the present study, the isthmo-optic complex (IOC) of the Chilean Tinamou forms part of a comparable general circuitry as the isthmo-optic nucleus (ION) of Neognathae: It receives afferents from tecto-IOC neurons in the TeO and sends centrifugal visual efferents to the retina. In contrast to Neognathae with a well-developed ION, the tecto-IOC axons end as divergent terminals in the IOC, as do the retinopetal IOC fibers in the retina. The retinal targets of the IOC continue to be unknown, but the centrifugal projection seems to be asymmetrical as in Neognathae, since it is confined to the equatorial and ventral retina [Color figure can be viewed at wileyonlinelibrary.com]

indicated that the centrifugal fibers and terminals were topographically confined to the equatorial to ventral retina.

5 | DISCUSSION

The present study provides for the first time a detailed description of the centrifugal visual system of a palaeognathous bird. We have analyzed its circuitry in the Chilean Tinamou (*Nothoprocta perdicaria*) by in vivo and in vitro neural tracing experiments, focusing on the main components which have been studied in various neognathous species for over a century. Our findings indicate that while the Tinamou lacks a well-developed ION, its centrifugal visual neurons form a congregate IOC which receives divergent afferents from the optic tectum (TeO) and sends a prominent but exclusively divergent projection to the retina (Figure 10). Thus, similar to the Neognathous ION, the Palaeognathous IOC mediates a feedback circuit between the TeO and the retina. The elements of this centrifugal visual system circuitry, however, have notable structural and organizational differences. In particular, the multipolar morphology of the IOC neurons and their divergent terminals in the retina show parallels to the "ectopic centrifugal neurons" which lie outside the neognathous ION. These findings, which will now be discussed in detail, may have important implications for the understanding of evolution, development, and function of the centrifugal visual system, and lead the way for future comparative studies.

5.1 | The istmo-optic complex

An ION is clearly present in most neognathous birds (Gutiérrez-Ibáñez et al., 2012, 2014). It characteristically consists of small monopolar neurons ~15 μm in diameter, which in Neognathae with well-developed ION form a lamina around a central neuropil containing their dendrites (Clarke & Caranzano, 1985; Cowan, 1970; Güntürkün, 1987; Li & Wang, 1999). The morphologically different ectopic centrifugal neurons, which lie outside the proper ION, are more heterogeneous in size and generally multipolar (Clarke & Cowan, 1975; Cowan & Clarke, 1976; Hayes & Webster, 1981; Li & Wang, 1999; Médina, Repérant, Miceli, Bertrand, & Bennis, 1998; O'Leary & Cowan, 1982; Weidner, Desroches, Repérant, Kirpitchnikova, & Miceli, 1989; Weidner, Repérant, Desroches, Miceli, & Vesselkin, 1987; Wolf-Oberhollenzer, 1987). The ION presents a high variety of morphologies with different levels of complexity, but in most species (with some noteworthy exceptions such as Procellariiformes and Pelicaniformes) it is at least clearly distinguishable as a nucleus (Gutiérrez-Ibáñez et al., 2012). Therefore, the reported complete absence of an ION in Palaeognathae, represented by the Southern brown kiwi *Apteryx australis* (Craigie, 1930), the ostrich *Struthio camelus* (Verhaart, 1971), and more recently the Chilean Tinamou (Gutiérrez-Ibáñez et al., 2012), has been striking. However, our previous (Krabichler et al., 2015) and present data have shown that intraocular tracer injections in the Chilean Tinamou retrogradely label numerous centrifugal visual neurons in the dorsal isthmus, ~4100 contralaterally and 300 ipsilaterally projecting cells on each side (Krabichler et al., 2015). While their location suggests that they correspond to the neognathous ION, they do not form a distinct nucleus but a diffuse cellular group, which we have termed IOC. The finding that Palaeognathae do in fact possess a substantial number of IO neurons, although differently organized than an ION, is interesting. Foremost, the relatively large and multipolar IOC neurons resemble neognathous ectopic centrifugal neurons rather than ION neurons. Since also crocodiles, the closest living relatives of birds (Figure 2), possess exclusively "ectopic-like" centrifugal neurons (Ferguson, Mulvanny, & Brauth, 1978; Médina, Repérant, Ward, & Miceli, 2004), we previously hypothesized that the Tinamou's IOC neurons may correspond to the "ectopic-like" centrifugal neurons of the sauropsidian ancestors, while the "true" ION first evolved in Neognathae after their divergence from the Palaeognathae (Krabichler et al., 2015).

On the other hand, the IOC of the Chilean Tinamou has a much more congregate organization than the IO neurons of crocodiles, which lie dispersed over a widespread area around the isthmus (Médina et al., 2004). In fact, the dense IOC "core" region which contains the majority of the centrifugal neurons, is somewhat reminiscent of the neognathous ION, while relatively few neurons lie scattered over a wider area like ectopic centrifugal neurons (Figure 4b,c). Thus, the question of how IOC, ION and ectopic centrifugal neurons relate to one another may not have a simple answer. In Neognathae, developmental evidence suggests that ION neurons and ectopic centrifugal neurons arise from the same embryonic precursors: They are generated over the same time period (Clarke, 1982), are subjected to the same degree of naturally occurring cell death during embryogenesis (O'Leary & Cowan,

1982), and initially have the same morphology, which subsequently changes within the developing ION by dendritic reorientation and cytolamination (Clarke & Kraftsik, 1996). The differentiation into the segregated populations of ION and ectopic centrifugal neurons might therefore be epigenetically induced by different morphogenetic influences resulting from their relations and milieu interactions, rather than because they represent inherently separated cell lineages (O'Leary & Cowan, 1982). Accordingly, the Tinamou's IOC could constitute an "undifferentiated" organizational layout in which no dendritic reorientation and cytolamination occur, rather than represent either an "ectopic centrifugal neurons" or an "ION lineage." Clearly, this issue cannot be resolved based solely on morphology, but needs to consider more meaningful comparative criteria. In the present study we have focused on the hodology of the palaeognathous centrifugal visual system to determine whether its IOC has comparable connections as the neognathous ION.

5.2 | Tectal afferents to the IOC

The ION of Neognathae receives its major afferents from tecto-ION neurons in the TeO. In the chicken, quail, and pigeon, these neurons form a narrowly spaced monolayer in L9–10 of the TeO (Crossland & Hughes, 1978; Miceli et al., 1993, 1997; Uchiyama et al., 1996; Uchiyama & Watanabe, 1985; Woodson et al., 1991;) and their axons are thought to make one-on-one contacts on single ION cells (Li, Hu, & Wang, 1999; Uchiyama et al., 1996; Woodson et al., 1991). In addition, the ION/ectopic centrifugal neurons of neognathous birds possess extratectal afferents (Médina et al., 1998; Miceli et al., 1997, Miceli, Repérant, Bertrand, & Rio, 1999, Miceli, Repérant, Rio, Hains, & Medina, 2002; Repérant et al., 1989), which according to results from transneuronal tracing with RITC (Miceli et al., 1997) and more recently transsynaptic viral vectors (Mundell et al., 2015), originate in several brainstem regions such as the mesencephalic reticular formation, pontine reticular formation, and ventral tegmental area (formerly ventral area of Tsai; Reiner et al., 2004). However, it is still unknown if the extratectal afferents project to ION cells or ectopic centrifugal neurons or both.

Our tracer injections into the TeO of the Chilean Tinamou showed a clear tectal projection to the IOC (Figure 5). Moreover, the tecto-IOC fibers appeared to take the same path as the tecto-ION fibers in Neognathae, which converge into the tecto-isthmal tract ventral to the third (i.e., tectal) ventricle (Cowan, 1970; Uchiyama et al., 1996; Uchiyama & Watanabe, 1985; Woodson et al., 1991). However, unlike the topographically confined ("convergent") tecto-ION terminals described in Neognathae (Uchiyama et al., 1996; Wylie, Gutiérrez-Ibáñez, Pakan, & Iwaniuk, 2009), tecto-IOC axons were thin and possessed "divergent" varicose terminals, which ramified over wider areas within the IOC core (Figure 5e,g). Due to this widespread configuration, the terminals from each tecto-IOC neuron may contact various IOC neurons. Interestingly, no tectal terminals were observed in the areas surrounding the IOC core, even though they contained many radially extending IOC dendrites (Figure 4b,c). This might indicate that extratectal rather than tectal afferents project onto these dendrites. However, the lack of tectal fibers in these regions might also be a result of the small sizes of the tectal injections. In the future, this issue could be resolved with the help of retrogradely transsynaptic viral vectors.

We identified the tectal neurons giving rise to the tecto-IOC projection by tracer injections into the IOC. Neurons were retrogradely labeled in both intermediate (L10a) and deep (L13–15) layers. The L13–15 neurons most likely represented projections to tegmental structures such as the field A8 (formerly anterior portion of locus coeruleus; Reiner et al., 2004), or pathways which traverse peri-IOC regions such as certain descending projections (Reiner & Karten, 1982) or the tecto-tegmento-tectal pathway (Stacho, Letzner, Theiss, Manns, & Güntürkün, 2016). In fact, labeled L13–15 neurons have also been reported in chicken and pigeons following injections into tegmental areas ventrolateral to the ION, while injections confined to the ION never labeled such cells (Woodson et al., 1991).

By all evidence, the cells labeled in L10a (Figure 6) represented the tecto-IOC neurons. (i) They were located in a similar layer as their neognathous counterparts and likewise appeared to form a regularly spaced monolayer. (ii) They were consistently found in all successful IOC injections. Control cases with injections outside the IOC failed to label any neurons in intermediate tectal layers (i.e., L8–12), analogous to what has been reported in Neognathae (Reiner & Karten, 1982). (iii) Axons of the L10a neurons were sometimes observed with collateral terminals in deep tectal layers L11–12 (Figure 6f), which is similar to findings in the quail (Uchiyama, 1989; Uchiyama et al., 1996; Uchiyama & Watanabe, 1985). (iv) The tectal injections which labeled terminals in the IOC were centered in intermediate tectal layers.

The tecto-IOC neurons of the Chilean Tinamou show some differences from their counterparts in Neognathae. First, they appear to have a sparser distribution. The tecto-ION neurons of the chicken (Crossland & Hughes, 1978; Woodson et al., 1991), the quail (Uchiyama et al., 1996; Uchiyama & Watanabe, 1985), and the pigeon (Miceli et al., 1993; Woodson et al., 1991), lie in a narrowly spaced monolayer around the TeO. In accordance with their assumed one-on-one projection to ION cells, their total number has been estimated to 7000–10,000 in the quail (Uchiyama et al., 1996), 9,500 in the chicken (Clarke, Rogers, & Cowan, 1976), and 12,000 in the pigeon (Woodson et al., 1991). Our results suggest that the Chilean Tinamou tecto-IOC neurons represent a smaller population with broader inter-cell spacing (100–300 μm; Figure 6) than the tecto-ION neurons of Neognathae such as the quail (50–100 μm; Uchiyama et al., 1996) and the pigeon (30–175 μm; Woodson et al., 1991). Though our data do not permit us to provide a confident estimation of the number of tecto-IOC neurons, they could (by interpolating the numbers and intercell spacing in Neognathae) amount to a few thousand. It should be noted that even though this may suggest similar numbers of tecto-IOC and IOC neurons in the Tinamou (see above), a precisely tuned 1:1 ratio as in Neognathae is unlikely, because the tecto-IOC projection is divergent rather than 1-on-1 as the tecto-ION projection.

Another difference regards morphology. The tecto-ION cells of Neognathae such as quail (Uchiyama et al., 1996), pigeon (Woodson et al., 1991), and chicken (Heyers, Luksch, & Redies, 2004) are multipolar, with a conspicuous "willow-like" appearance, which results from

thick dendrites bending downward to deeper layers and arranging themselves into radial columns (Uchiyama & Watanabe, 1985). While the Tinamou's tecto-IOC neurons are also multipolar, their dendrites are not arranged in columns but extend horizontally and obliquely over wider tectal areas (Figure 6). Interestingly, these dendrites often spread toward neighboring tecto-IOC neurons, which might permit their population to functionally cover the entire TeO with their receptive fields.

All evidence combined suggests that the palaeognathous Chilean Tinamou possesses a TeO-IOC projection originating from a population of tectal neurons in L10a. Their morphological dissimilarities from the neognathous tecto-ION neurons could be regarded as evidence that they do not correspond to those but perhaps to a different lineage of neurons projecting to the ectopic centrifugal neurons. However, there is only limited evidence for a "tecto-ectopic" projection in Neognathae (Clarke, 1985; O'Leary & Cowan, 1982; Uchiyama et al., 1996; Woodson et al., 1991), and the identity of the putative "tecto-ectopic" neurons is unknown. By contrast, the tecto-IOC and tecto-ION neurons could indeed be homologous, and their main differing characters, for example the wide-spread dendrites of the tecto-IOC neurons, could be morphogenetically induced by factors such as their wider intercell spacing. In any case, the connectivity between the TeO and the centrifugal visual system seems to be an ancestral characteristic of archosauria (Figure 2), since there is evidence that the IO neurons of crocodiles receive a tectal projection. Tracer injections into the TeO of *Caiman crocodilus* have been reported to label fibers and some terminals in its IO area (Ferguson et al., 1978). However, the tectal fibers have not been conclusively shown to contact the IO neurons, and the putative tecto-IO neurons have so far not been identified. The tecto-ION neurons of pigeons can be conveniently labeled by retrograde transneuronal transport of intraocularly injected RITC (Miceli et al., 1997, 1993), while this has unfortunately failed both in crocodiles (Médina et al., 2004) as well as in preliminary experiments performed by us in the Chilean Tinamou. Possibly, very dense connections are necessary for detectable transneuronal RITC transport to occur. In the future, retrograde trans-synaptic viral vector tracing may facilitate comparative studies of the afferents to centrifugal visual neurons in birds and reptiles (Mundell et al., 2015).

5.3 | Centrifugal visual fibers to the retina

In Neognathae such as the chicken (Lindstrom et al., 2009), Japanese quail (Uchiyama & Ito, 1993), and pigeon (Hayes & Holden, 1983; Woodson et al., 1995), centrifugal fibers from both ION cells and ectopic centrifugal neurons project to the retina via the isthmo-optic tract (Catsicas, Catsicas, & Clarke, 1987b; Cowan & Powell, 1963; Crossland & Hughes, 1978; Galifret et al., 1971; Hayes & Webster, 1981; Wallenberg, 1898) and terminate within the exterior segment of the IPL or at the interior edge of the INL (Chmielewski et al., 1988; Dogiel, 1895). ION axons form striking "convergent" terminals (Fischer & Stell, 1999; Lindstrom et al., 2009; Morgan et al., 1994; Nickla et al., 1994) on "association amacrine cells" (Ramón y Cajal, 1893, 1911; Mariani, 1982; Uchiyama & Stell, 2005), which are readily identifiable by their striking morphology and strong staining for Parvalbumin and NADPH-diaphorase (Fischer & Stell, 1999; Lindstrom et al., 2009, 2010; Uchiyama & Stell, 2005; Wilson et al., 2011; present results, Figure 7b). The axons of ectopic centrifugal neurons form "divergent" terminals, which widely ramify in the IPL over a greater area of retinal space (Chmielewski et al., 1988; Dogiel, 1895; Fritzsch et al., 1990; Hayes & Holden, 1983; Lindstrom et al., 2009; Maturana & Frenk, 1965; Uchiyama & Ito, 1993; Woodson et al., 1995;). They have been suggested to contact displaced ganglion cells (Dogiel, 1895; Hayes & Holden, 1983; Maturana & Frenk, 1965; Nickla et al., 1994) and "flat" amacrine cells (Dogiel, 1895; Maturana & Frenk, 1965).

In the Chilean Tinamou retina, we exclusively found "divergent" centrifugal visual fibers by in vitro as well as in vivo tracing experiments. The absence of the "convergent" type was corroborated by the lack of any strongly-labeled NADPH-diaphorase-positive structures in the INL/IPL that would resemble the pericellular terminal nests in the chicken (Figure 7d). The divergent terminals formed a dense varicosity-rich mesh in equatorial and ventral parts of the retina (Figures 8 and 9a), similar to the divergent terminals of ectopic centrifugal neurons in the pigeon (Woodson et al., 1995; compare their figure 15 with our Figure 9a). Within the retina, the terminals were located in the outermost IPL and partially entered the innermost INL (Figures 8d and 9c), which was in the in vitro tracings (Figure 8) identified by Parvalbumin-positive amacrine cells (Fischer & Stell, 1999; Hamano et al, 1990; Sanna et al., 1992) and retrogradely labeled displaced ganglion cells (Karten, Fite, & Brecha, 1977; Wilson et al., 2011). Interestingly, in Neognathae only the convergent ION terminals have been described to enter the INL (Dowling & Cowan, 1966; Lindstrom et al., 2009; Ramón y Cajal, 1911), while the divergent ones remain in the IPL (Chmielewski et al., 1988; Dogiel, 1895; Fritzsch et al., 1990).

The findings that the IOC retinal terminals in the Chilean Tinamou have a divergent morphology and do not form prominent NADPH-diaphorase-positive terminals on Parvalbumin-positive AACs, could be seen as supporting the notion that the IOC neurons correspond to ectopic centrifugal neurons of Neognathae. Unfortunately, our data have not revealed the actual targets of the IOC fibers in the retina. Because the IPL sublamina where the displaced ganglion cells dendrites ramify contained only few (if any) centrifugal terminals (Figure 8d), displaced ganglion cells are unlikely to be the major targets.

An intriguing question is whether the Tinamou possesses cells which correspond to the neognathous AACs but receive divergent IOC terminals instead of convergent ones. As one possibility, such palaeognathous AACs could be among the Tinamou's NADPH-diaphorase- and Parvalbumin-positive INL neurons, but morphologically different from chicken AACs. However, very few Parvalbumin-positive processes are found in sublamina I of the Tinamou's IPL (Figure 7a), although this is in chicken the main distribution zone of the AAC processes and therefore strongly labeled (Figure 7b; Fischer & Stell, 1999; Hamano et al., 1990; Sanna et al., 1992). Another possibility could be that palaeognathous AACs exist, but either ancestrally or due to secondary loss do not express both Parvalbumin and NADPH diaphorase (or at least not sufficiently for detection by histochemical methods). Finally, AACs might be an evolutionary novelty only found in Neognathae.

This also leads to the question how the neognathous AACs, the convergent centrifugal fibers, and the intimate connection between the two originally evolved. It should be noted that divergent centrifugal visual fibers terminating at the border of IPL and INL are the prevalent configuration in almost all vertebrates (Repérant et al., 2007, p. 171), including humans (Repérant & Gallego, 1976). Convergent fibers, on the other hand, have only been reported in neognathous birds with a well-developed ION. Interestingly, their connection with the AACs is not entirely exclusive: In the pigeon, the convergent ION fibers form loose pericellular nests with many collaterals (Dogiel, 1895; Dowling & Cowan, 1966; Hayes & Holden, 1983; Maturana & Frenk, 1965; Woodson et al., 1995), and even the dense pericellular nests in the chicken split off side branches, which form synaptic boutons on other unknown targets (Lindstrom et al., 2009).

Thus it is conceivable that the convergent terminals first emerged in Neognathae by reinforcing a specific connection (i.e., with the AACs) out of a pool of originally existing "divergent" connections, along with the differentiation of the centrifugal visual system into an ECN and an ION pathway. Consequently, rather than being a completely *de novo* evolutionary innovation of Neognathae, cells homologous to the AACs could exist in Palaeognathae such as the Chilean Tinamou, and perhaps even in crocodiles. Furthermore it is possible that the high level of plasticity, which is indicated by the variability of the ION among Neognathae (Gutiérrez-Ibáñez et al., 2012), is retained at all levels of the avian centrifugal visual system. Thus, in Neognathae with poorly developed or absent ION such as storks (Showers & Lyons, 1968) and sea birds (Procellariiformes and Pelicaniformes; Gutiérrez-Ibáñez et al., 2012), a reversal to an undifferentiated centrifugal visual system configuration similar as in the Chilean Tinamou might again be found, including the terminals and their targets in the retina. In the future, broad comparative studies of the retinal centrifugal visual system components in Neognathous and Palaeognathous birds as well as crocodiles could give new insights into evolutionary and developmental principles of the avian centrifugal visual system.

5.4 | Implications for functional hypotheses of the centrifugal visual system

The striking nature of the avian centrifugal visual system has led to a long-standing debate about its functional and behavioral significance (Repérant et al., 1989) and many hypotheses have been put forward (reviewed in Wilson & Lindstrom, 2011). Previous studies have almost exclusively focused on Neognathae with well-developed, specialized ION. Their centrifugal visual system is generally thought to constitute an excitatory feedback loop (Li et al., 1999; Pearlman & Hughes, 1976) with a well-defined topography as demonstrated both anatomically (Crossland & Hughes, 1978; McGill et al., 1966a, 1966b; Uchiyama et al., 1996; Wylie et al., 2009) and physiologically (Holden & Powell, 1972; Li, Xiao, Fu, & Wang, 1998; Miles, 1972; Uchiyama, Nakamura, & Imazono, 1998). Functionally, this presumably results in a considerable spatial resolution due to the high number of ION neurons, "one-on-one" projecting tecto-ION neurons, and "one-on-one" convergent ION fibers to retinal AACs. However, the ION size and complexity among Neognathae are highly variable. In fact, small or indistinguishable ION are found in many species that are neither basal nor necessarily closely related (Feyerabend, Malz, & Meyer, 1994; Gutiérrez-Ibáñez et al., 2012; Shortess & Klose, 1975; Weidner et al., 1987).

The Chilean Tinamou represents an excellent model for studying a centrifugal visual system with an undeveloped ION and only divergent fibers. While the participation of the TeO in the circuit and the congregate IOC organization suggest that the system is in some way topographically organized, the divergent connections between its components should result in a comparatively low spatial resolution. This makes it unlikely that the Chilean Tinamou's centrifugal visual system is involved in any spatially accurate mechanisms of visual attention. The well-differentiated ION has for instance been suggested to represent an adaptation in ground-feeding birds, for functions such as retinal spot-lighting or attention scanning during pecking (Galifret et al., 1971; Holden, 1990; Marín et al., 1990; Uchiyama, 1989; Uchiyama et al., 1998; Uchiyama & Barlow, 1994). Although the Chilean Tinamou is an exclusively ground-living and ground-feeding bird (Cabot, 1992), it is improbable that its IOC is involved in such tasks. However, because the IOC projection targets only the equatorial to ventral retina similar to both the convergent and divergent fibers in Neognathae (Lindstrom et al., 2009; Woodson et al., 1995), it might in some way serve for switching attention between coarse retinal regions such as from ventral to dorsal (Clarke, Gyger, & Catsicas, 1996; Gutiérrez-Ibáñez et al., 2012); or for some rough form of covert spatial attention by "illuminating" retinal regions without eye-head movements (Ohno & Uchiyama, 2009). Wilson & Lindstrom (2011) suggested on grounds of the asymmetrical centrifugal projection that well-developed ION could serve for detecting aerial predators by switching attention from shadows on the ground toward the sky. However, this hypothesis is contradicted by the existence of many aerially predated Neognathae with small ION (Gutiérrez-Ibáñez et al., 2012). Likewise, the Chilean Tinamou has not developed a more specialized ION despite being heavily preyed on by diurnal raptors (Figueroa & Corales, 1999; Jiménez & Jaksić, 1989).

In the end, such functional comparisons between the Chilean Tinamou and Neognathae must consider the different organization of the ION-based and IOC-based centrifugal visual system, which probably imply different functions as well. Due to the structural similarities between the IOC and the neognathous "ectopic centrifugal neurons", the IOC might even possess a functional role similar to those rather than the ION. While the ectopic centrifugal neurons have unfortunately been barely investigated, recent studies with lesion experiments have suggested that the chicken centrifugal visual system (especially the ectopic centrifugal neurons) might play a role in regulating eye development (Dillingham et al., 2013, 2017). In order to test this hypothesis, similar studies could be performed in the Tinamou.

Apart from that, the Tinamou could serve as a model for studying the functional role of extratectal afferents to the centrifugal visual system, which may for example contact the numerous radially extending IOC dendrites. The structures into which these dendrites extend could give a first hint toward their possible roles. For example, many

of them are found in the central gray, which has recently been proposed as being implicated in tonic immobility to predator attacks in pigeons (Melleu, Lino-de-Oliveira & Marino-Neto, 2017). Interestingly, a striking behavior of the Tinamou is that it freezes when in danger (and only as a last resort jumps up and flies forcefully away; Cabot, 1992). Thus, IOC dendrites might receive projections from central gray neurons or their affiliated circuits, modulating the centrifugal visual system during tonic immobility, possibly affecting visual attention. While this is of course very speculative, it may be worthwhile to study the radially extending IOC dendrites and the extratectal IOC afferents in detail.

Our present study stresses the importance of comparative neurobiology. Comparison can reveal the context in which neuronal circuits have evolved, and this is ultimately also important for understanding their functions. With respect to the centrifugal visual system, we suggest to widen the range of avian (and reptilian) model organisms, in order to study its plasticity and how it may correlate with phylogeny as well as different life-styles and behaviors. Palaeognathous birds hereby represent an important link due to their long evolutionary divergence from Neognathae, and in this respect the Chilean Tinamou is becoming increasingly established as a valuable model for comparative neurobiology (Corfield et al., 2015; Krabichler et al., 2015).

ACKNOWLEDGMENTS

We wish to thank Solano Henriquez, Elisa Sentis, Elmar Jocham, and Birgit Seibel for their help and excellent technical assistance. We are grateful toward Prof. Jorge Mpodozis, Dr. Cristian González-Cabrera, and Cristian Morales for providing valuable help during some of the experiments.

CONFLICT OF INTEREST

The authors declare no conflict of interest.

AUTHOR CONTRIBUTION

All authors had full access to all the data in the study and take responsibility for the integrity of the data and the accuracy of the data analysis. Study concept and design: QK, TVZ, GM, HL. Acquisition of data: All in vivo and in vitro experiments were conducted at the Universidad de Chile. Most of them were done by QK during several research visits, while a few complementary experiments were done by MF, DC, TVZ and GM. Histology and histochemistry were performed by QK at the Universidad de Chile and at the Technische Universität München in Germany. Analysis and interpretation of data: QK, TVZ, CG, HL, GM. Drafting of the manuscript: QK. Critical revision of the manuscript for important intellectual content: TVZ, CG, HL, GM. Obtained funding: GM, HL. Study supervision: HL and GM.

REFERENCES

Adams, J. C. (1992). Biotin amplification of biotin and horseradish peroxidase signals in histochemical stains. *Journal of Histochemistry & Cytochemistry*, *40*, 1457–1463. doi:10.1177/40.10.1527370

Angelucci, A., Clascá, F., & Sur, M. (1996). Anterograde axonal tracing with the subunit B of cholera toxin: **A** highly sensitive immunohistochemical protocol for revealing fine axonal morphology in adult and neonatal brains. *Journal of Neuroscience Methods*, *65*, 101–112. doi:10.1016/0165-0270(95)00155-7

Bobrow, M. N., Harris, T. D., Shaughnessy, K. J., & Litt, G. J. (1989). Catalyzed reporter deposition, a novel method of signal amplification application to immunoassays. *Journal of Immunological Methods*, *125*, 279–285. doi:10.1016/0022-1759(89)90104-X

Brusatte, S. L., O'Connor, J. K., & Jarvis, E. D. (2015). The origin and diversification of birds. *Current Biology*, *25*, R888–R898. doi:10.1016/j.cub.2015.08.003

Cabot, J. (1992). Family Tinamidae (Tinamous). In J. Del Hoyo, A. Elliott, & J. Sargatal (Eds.), Handbook of the birds of the world: Ostrich to ducks (Vol. *1*, pp. 112–138).Barcelona: Lynx Edicions.

Catsicas, S., Catsicas, M., & Clarke, P. G. H. (1987a). Long-distance intraretinal connections in birds. *Nature*, *326*, 186–187. doi:10.1038/326186a0

Catsicas, S., Thanos, S., & Clarke, P. G. H. (1987b). Major role for neuronal death during brain development: Refinement of topographical connections. *Proceedings of the National Academy of Sciences USA*, *84*, 8165–8168.

Chmielewski, C. E., Dorado, M. E., Quesada, A., Geniz-Galvez, J. M., & Prada, F. A. (1988). Centrifugal fibers in the chick retina. *Anatomia, Histologia, Embryologia*, *17*, 319–327. doi:10.1111/j.1439-0264.1988.tb00570.x

Claramunt, S., & Cracraft, J. (2015). A new time tree reveals Earth history's imprint on the evolution of modern birds. *Science Advances*, *1*, e1501005. doi:10.1126/sciadv.1501005

Clarke, P. G. H. (1982). The generation and migration of the chick's isthmic complex. *Journal of Comparative Neurology*, *207*, 208–222. doi:10.1002/cne.902070303

Clarke, P. G. H. (1985). Neuronal death during development in the isthmo-optic nucleus of the chick: Sustaining role of afferents from the tectum. *Journal of Comparative Neurology*, *234*, 365–379. doi:10.1002/cne.902340307

Clarke, P. G. H., & Caranzano, F. (1985). Dendritic development in the isthmo-optic nucleus of chick embryos. *Developmental Neuroscience*, *7*, 161–169. doi:10.1159/000112284

Clarke, P. G. H., & Cowan, W. M. (1975). Ectopic neurons and aberrant connections during neural development. *Proceedings of the National Academy of Sciences USA*, *72*, 4455–4458.

Clarke, P. G. H., Gyger, M., & Catsicas, S. (1996). A centrifugally controlled circuit in the avian retina and its possible role in visual attention switching. *Visual Neuroscience*, *13*, 1043–1048. doi:10.1017/S0952523800007690

Clarke, P. G. H., & Kraftsik, R. (1996). Dendritic reorientation and cytolamination during the development of the isthmo-optic nucleus in chick embryos. *Journal of Comparative Neurology*, *365*, 96–112. doi:10.1002/(SICI)1096-9861(19960129)365:1<96::AID-CNE8>3.0.CO;2-E

Clarke, P. G. H., Rogers, L. A., & Cowan, W. M. (1976). The time of origin and the pattern of survival of neurons in the isthmo-optic nucleus of the chick. *Journal of Comparative Neurology*, *167*, 125–141. doi:10.1002/cne.901670202

Corfield, J. R., Kolominsky, J., Marín, G. J., Craciun, I., Mulvany-Robbins, B. E., Iwaniuk, A. N., & Wylie, D. R. (2015). Zebrin II expression in the cerebellum of a paleognathous bird, the chilean tinamou (*Nothoprocta perdicaria*). *Brain, Behavior and Evolution*, 85(2), 94–106. doi:10.1159/000380810

Cowan, W., & Clarke, P. (1976). The development of the isthmo-optic nucleus. *Brain, Behavior and Evolution*, *13*, 345–375.

Cowan, W. M. (1970). Centrifugal fibres to the avian retina. *British Medical Bulletin*, *26*, 112–118.

Cowan, W. M., Adamson, L., & Powell, T. P. S. (1961). An experimental study of the avian visual system. *Journal of Anatomy*, *95*, 545–563.

Cowan, W. M., & Powell, T. P. S. (1963). Centrifugal fibres in the avian visual system. *Proceedings of the Royal Society of London. Series B, Biological Sciences 158*, 232–252. doi:10.2307/90428

Craigie, E. H. (1930). Studies on the brain of the kiwi (Apteryx australis). *Journal of Comparative Neurology*, *49*, 223–357. doi:10.1002/cne.900490202

Crossland, W. J., & Hughes, C. P. (1978). Observations on the afferent and efferent connections of the avian isthmo-optic nucleus. *Brain Research*, *145*, 239–256. doi:10.1016/0006-8993(78)90860-0

Dillingham, C. M., Guggenheim, J. A., & Erichsen, J. T. (2013). Disruption of the centrifugal visual system inhibits early eye growth in chicks. *Investigative Opthalmology & Visual Science*, *54*, 3632. doi:10.1167/iovs.12-11548

Dillingham, C. M., Guggenheim, J. A., & Erichsen, J. T. (2017). The effect of unilateral disruption of the centrifugal visual system on normal eye development in chicks raised under constant light conditions. *Brain Structure and Function*, 222(3), 1315–1330. doi:10.1007/s00429-016-1279-9

Dogiel, A. S. (1895). Die retina der Vögel. *Archiv für mikroskopische Anatomie*, *44*, 622–648. doi:10.1007/BF02934032

Dowling, J. E., & Cowan, W. M. (1966). An electron microscope study of normal and degenerating centrifugal fiber terminals in the pigeon retina. *Zeitschrift für Zellforschung*, *71*, 14–28. doi:10.1007/BF00339827

Ferguson, J. L., Mulvanny, P. J., & Brauth, S. E. (1978). Distribution of neurons projecting to the retina of *Caiman crocodilus*. *Brain, Behavior and Evolution*, *15*, 294–306.

Feyerabend, B., Malz, C. R., & Meyer, D. L. (1994). Birds that feed-on-the-wing have few isthmo-optic neurons. *Neuroscience Letters*, *182*, 66–68. doi:10.1016/0304-3940(94)90207-0

Figueroa, R. A., & Corales, E. S. (1999). Food habits of the Cinereous Harriers (*Circus cinereus*) in the Araucanía, southern Chile. *Journal of Raptor Research*, *33*, 264–267.

Fischer, A. J., & Stell, W. K. (1999). Nitric oxide synthase-containing cells in the retina, pigmented epithelium, choroid, and sclera of the chick eye. *Journal of Comparative Neurology*, *405*, 1–14. doi:10.1002/(SICI)1096-9861(19990301)405:1 < 1::AID-CNE1 > 3.0.CO;2-U

Fritzsch, B., de Caprona, M.-D. C., & Clarke, P. G. H. (1990). Development of two morphological types of retinopetal fibers in chick embryos, as shown by the diffusion along axons of a carbocyanine dye in the fixed retina. *Journal of Comparative Neurology*, *300*, 405–421. doi:10.1002/cne.903000310

Galifret, Y., Condé-Courtine, F., Repérant, J., & Servière, J. (1971). Centrifugal control in the visual system of the pigeon. *Vision Research 11*, 185–200. doi:10.1016/0042-6989(71)90039-3

Giloh, H., & Sedat, J. W. (1982). Fluorescence microscopy: reduced photobleaching of rhodamine and fluorescein protein conjugates by n-propyl gallate. *Science*, *217*, 1252–1255. doi:10.1126/science.7112126

Green, M. A., Sviland, L., Malcolm, A. J., & Pearson, A. D. (1989). Improved method for immunoperoxidase detection of membrane antigens in frozen sections. *Journal of Clinical Pathology*, *42*, 875–880. doi:10.1136/jcp.42.8.875

Güntürkün, O. (1987). A Golgi study of the isthmic nuclei in the pigeon (*Columba livia*). *Cell and Tissue Research*, *248*, 439–448. doi:10.1007/BF00218211

Gutiérrez-Ibáñez, C., Iwaniuk, A. N., Lisney, T. J., Faunes, M., Marín, G. J., & Wylie, D. R. (2012). Functional implications of species differences in the size and morphology of the isthmo optic nucleus (ION) in birds. *PLoS ONE*, *7*, e37816. doi:10.1371/journal.pone.0037816

Gutiérrez-Ibáñez, C., Iwaniuk, A. N., Moore, B. A., Fernández-Juricic, E., Corfield, J. R., Krilow, J. M., Kolominsky, J., & Wylie, D. R. (2014). Mosaic and concerted evolution in the visual system of birds. *PLoS ONE*, *9*, e90102. doi:10.1371/journal.pone.0090102

Hamano, K., Kiyama, H., Emson, P. C., Manabe, R., Nakauchi, M., & Tohyama, M. (1990). Localization of two calcium binding proteins, calbindin (28 kD) and parvalbumin (12 kD), in the vertebrate retina. *Journal of Comparative Neurology*, *302*, 417–424. doi:10.1002/cne.903020217

Hayes, B. P., & Webster, K. E. (1981). Neurones situated outside the isthmo-optic nucleus and projecting to the eye in adult birds. *Neuroscience Letters*, *26*, 107–112. doi:10.1016/0304-3940(81)90334-7

Hayes, D. B. P., & Holden, A. L. (1983). The distribution of centrifugal terminals in the pigeon retina. *Experimental Brain Research*, *49*, 189–197. doi:10.1007/BF00238579

Heyers, D., Luksch, H., & Redies, C. (2004). Selective synaptic cadherin expression by traced neurons of the chicken visual system. *Neuroscience*, *127*, 901–912. doi:10.1016/j.neuroscience.2004.05.023

Holden, A. L. (1968). The centrifugal system running to the pigeon retina. *The Journal of Physiology*, *197*, 199–219. doi:10.1113/jphysiol.1968.sp008555

Holden, A. L. (1990). Centrifugal pathways to the retina: which way does the "searchlight" point? *Visual Neuroscience*, *4*, 493–495. doi:10.1017/S0952523800005241

Holden, A. L., & Powell, T. P. S. (1972). The functional organization of the isthmo-optic nucleus in the pigeon. *The Journal of Physiology*, *223*, 419–447. doi:10.1113/jphysiol.1972.sp009856

Jarvis, E. D., Mirarab, S., Aberer, A. J., Li, B., Houde, P., Li, C., . . ., Zhang, G. (2014). Whole-genome analyses resolve early branches in the tree of life of modern birds. *Science*, *346*, 1320–1331. doi:10.1126/science.1253451

Jiménez, J. E., & Jaksić, F. M. (1989). Biology of the austral pygmy-owl. *The Wilson Bulletin*, *101*, 377–389. doi:10.2307/4162747.

Karten, H. J., Fite, K. V., & Brecha, N. (1977). Specific projection of displaced retinal ganglion cells upon the accessory optic system in the pigeon (*Columbia livia*). *Proceedings of the National Academy of Sciences USA*, *74*, 1753–1756.

Krabichler, Q., Vega-Zuniga, T., Morales, C., Luksch, H., & Marín, G. J. (2015). The visual system of a Palaeognathous bird: Visual field, retinal topography and retino-central connections in the Chilean Tinamou (*Nothoprocta perdicaria*). *Journal of Comparative Neurology*, *523*, 226–250. doi:10.1002/cne.23676

Li, J. L., Xiao, Q., Fu, Y. X., & Wang, S. R. (1998). Centrifugal innervation modulates visual activity of tectal cells in pigeons. *Visual Neuroscience*, *15*, 411–415.

Li, W.-C., Hu, J., & Wang, S.-R. (1999). Tectal afferents monosynaptically activate neurons in the pigeon isthmo-optic nucleus. *Brain Research Bulletin*, *49*, 203–208. doi:10.1016/S0361-9230(99)00051-9

Li, W.-C., & Wang, S.-R. (1999). Morphology and dye-coupling of cells in the pigeon isthmo-optic nucleus. *Brain Behavior and Evolution*, *53*, 67–74. doi:10.1159/000006583

Lindstrom, S. H., Azizi, N., Weller, C., & Wilson, M. (2010). Retinal input to efferent target amacrine cells in the avian retina. *Visual Neuroscience*, *27*, 103–118. doi:10.1017/S0952523810000155

Lindstrom, S. H., Nacsa, N., Blankenship, T., Fitzgerald, P. G., Weller, C., Vaney, D. I., & Wilson, M. (2009). Distribution and structure of efferent synapses in the chicken retina. *Visual Neuroscience*, *26*, 215–226. doi:10.1017/S0952523809090063

Mariani, A. P. (1982). Association amacrine cells could mediate directional selectivity in pigeon retina. *Nature*, *298*, 654–655. doi:10.1038/298654a0

Marín, G. J., Letelier, J.-C., & Wallman, J. (1990). Saccade-related responses of centrifugal neurons projecting to the chicken retina. *Experimental Brain Research*, *82*, 263–270. doi:10.1007/BF00231246

Maturana, H. R., & Frenk, S. (1965). Synaptic connections of the centrifugal fibers in the pigeon retina. *Science*, *150*, 359–361. doi:10.1126/science.150.3694.359

McGill, J. I., Powell, T. P., & Cowan, W. M. (1966a). The organization of the projection of the centrifugal fibres to the retina in the pigeon. *Journal of Anatomy*, *100*, 35–49.

McGill, J. I., Powell, T. P., & Cowan, W. M. (1966b). The retinal representation upon the optic tectum and isthmo-optic nucleus in the pigeon. *Journal of Anatomy*, *100*, 5–33.

Médina, M., Repérant, J., Miceli, D., Bertrand, C., & Bennis, M. (1998). An immunohistochemical study of putative neuromodulators and transmitters in the centrifugal visual system of the quail (Coturnix japonica). *Journal of Chemical Neuroanatomy*, *15*, 75–95. doi:10.1016/S0891-0618(98)00034-9

Médina, M., Repérant, J., Ward, R., & Miceli, D. (2004). Centrifugal visual system of Crocodylus niloticus: A hodological, histochemical, and immunocytochemical study. *Journal of Comparative Neurology*, *468*, 65–85. doi:10.1002/cne.10959

Melleu, F. F., Lino-de-Oliveira, C., & Marino-Neto, J. (2017). The mesencephalic GCt–ICo complex and tonic immobility in pigeons (Columba livia): A c-Fos study. *Brain Structure and Function*, 222(3), 1253–1265. doi:10.1007/s00429-016-1275-0

Miceli, D., Repérant, J., Bavikati, R., Rio, J.-P., & Volle, M. (1997). Brainstem afferents upon retinal projecting isthmo-optic and ectopic neurons of the pigeon centrifugal visual system demonstrated by retrograde transneuronal transport of rhodamine β-isothiocyanate. *Visual Neuroscience*, *14*, 213–224. doi:10.1017/S0952523800011354

Miceli, D., Repérant, J., Bertrand, C., & Rio, J.-P. (1999). Functional anatomy of the avian centrifugal visual system. *Behavioural Brain Research*, *98*, 203–210. doi:10.1016/S0166-4328(98)00085-0

Miceli, D., Repérant, J., Marchand, L., & Rio, J.-P. (1993). Retrograde transneuronal transport of the fluorescent dye rhodamine β-isothiocyanate from the primary and centrifugal visual systems in the pigeon. *Brain Research*, *601*, 289–298. doi:10.1016/0006-8993(93)91723-6

Miceli, D., Repérant, J., Rio, J.-P., Hains, P., & Medina, M. (2002). Serotonin immunoreactivity in the retinal projecting isthmo-optic nucleus and evidence of brainstem raphe connections in the pigeon. *Brain Research*, *958*, 122–129. doi:10.1016/S0006-8993(02)03515-1

Miles, F. A. (1972). Centrifugal control of the avian retina. II. Receptive field properties of cells in the isthmo-optic nucleus. *Brain Research*, *48*, 93–113. doi:10.1016/0006-8993(72)90172-2

Morgan, I. G., Miethke, P., & Li, Z. K. (1994). Is nitric oxide a transmitter of the centrifugal projection to the avian retina? *Neuroscience Letters*, *168*, 5–7. doi:10.1016/0304-3940(94)90402-2

Mundell, N. A., Beier, K. T., Pan, Y. A., Lapan, S. W., Göz Aytürk, D., …, Cepko, C. L. (2015). Vesicular stomatitis virus enables gene transfer and transsynaptic tracing in a wide range of organisms. *Journal of Comparative Neurology*, 523(11), 1639–1663. doi:10.1002/cne.23761

Nickla, D. L., Gottlieb, M. D., Marín, G. J., Rojas, X., Britto, L. R. G., & Wallman, J. (1994). The retinal targets of centrifugal neurons and the retinal neurons projecting to the accessory optic system. *Visual Neuroscience*, *11*, 401–409. doi:10.1017/S0952523800001747

Ohno, H., & Uchiyama, H. (2009). Non-visually evoked activity of isthmo-optic neurons in awake, head-unrestrained quail. *Experimental Brain Research*, *194*, 339–346. doi:10.1007/s00221-009-1703-y

O'Leary, D. D. M., & Cowan, W. M. (1982). Further studies on the development of the isthmo-optic nucleus with special reference to the occurrence and fate of ectopic and ipsilaterally projecting neurons. *Journal of Comparative Neurology*, *212*, 399–416. doi:10.1002/cne.902120407

Papp, R. S., & Palkovits, M. (2014). Brainstem projections of neurons located in various subdivisions of the dorsolateral hypothalamic area: An anterograde tract-tracing study. *Frontiers in Neuroanatomy*, *8*, 34. doi:10.3389/fnana.2014.00034

Pearlman, A. L., & Hughes, C. P. (1976). Functional role of efferents to the avian retina. II. Effects of reversible cooling of the isthmo-optic nucleus. *Journal of Comparative Neurology*, *166*, 123–131. doi:10.1002/cne.901660109

Prum, R. O., Berv, J. S., Dornburg, A., Field, D. J., Townsend, J. P., Lemmon, E. M., & Lemmon, A. R. (2015). A comprehensive phylogeny of birds (Aves) using targeted next-generation DNA sequencing. *Nature*, 526(7574), 569–573. doi:10.1038/nature15697.

Ramamurthy, D. L., & Krubitzer, L. A. (2016). The evolution of whisker-mediated somatosensation in mammals: Sensory processing in barrelless S1 cortex of a marsupial, Monodelphis domestica. *Journal of Comparative Neurology*, *524*, 3587–3613. doi:10.1002/cne.24018

Ramón y Cajal, S. (1889). Sur la morphologie et les connexions des éléments de la rétine des oiseaux. *Anatomischer Anzeiger*, *4*, 111–121.

Ramón y Cajal, S., (1893). La rétine des vertébrés. *La Cellule*, *9*, 119–257.

Ramón y Cajal, S. (1911). *Histologie du système nerveux de l'homme et des vertébrés* (Vol. *II*) Paris: Maloine.

Reiner, A., & Karten, H. J. (1982). Laminar distribution of the cells of origin of the descending tectofugal pathways in the pigeon (Columba livia). *Journal of Comparative Neurology*, *204*, 165–187. doi:10.1002/cne.902040206

Reiner, A., Perkel, D. J., Bruce, L. L., Butler, A. B., Csillag, A., Kuenzel, W., … Jarvis, E. D. (2004). Revised nomenclature for avian telencephalon and some related brainstem nuclei. *Journal of Comparative Neurology*, *473*, 377–414. doi:10.1002/cne.20118

Repérant, J., & Gallego, A. (1976). Fibres centrifuges dans la rétine humaine. *Archives d'anatomie microscopique et de morphologie expérimentale*, *65*, 103–120.

Repérant, J., Médina, M., Ward, R., Miceli, D., Kenigfest, N. B., Rio, J. P., & Vesselkin, N. P. (2007). The evolution of the centrifugal visual system of vertebrates. A cladistic analysis and new hypotheses. *Brain Research Reviews*, *53*, 161–197. doi:10.1016/j.brainresrev.2006.08.004

Repérant, J., Miceli, D., Vesselkin, N. P., & Molotchnikoff, S. (1989). The centrifugal visual system of vertebrates: A century-old search reviewed. *International Review of Cytology*, *118*, 115–171.

Repérant, J., Ward, R., Miceli, D., Rio, J. P., Médina, M., Kenigfest, N. B., & Vesselkin, N. P. (2006). The centrifugal visual system of vertebrates: A comparative analysis of its functional anatomical organization. *Brain Research Reviews*, *52*, 1–57. doi:10.1016/j.brainresrev.2005.11.008

Sanna, P. P., Keyser, K. T., Deerink, T. J., Ellisman, M. H., Karten, H. J., & Bloom, F. E. (1992). Distribution and ontogeny of parvalbumin immunoreactivity in the chicken retina. *Neuroscience*, *47*, 745–751. doi:10.1016/0306-4522(92)90182-2

Schindelin, J., Arganda-Carreras, I., Frise, E., Kaynig, V., Longair, M., Pietzsch, T., … Cardona, A. (2012). Fiji: An open-source platform for biological-image analysis. *Nature Methods*, *9*, 676–682. doi:10.1038/nmeth.2019

Shortess, G. K., & Klose, E. F. (1975). The area of the nucleus isthmo-opticus in the American kestrel (Falco sparverius) and the red-tailed hawk (Buteo jamacensis). *Brain Research*, *88*, 525–531. doi:10.1016/0006-8993(75)90665-4

Showers, M. J. C., & Lyons, P. (1968). Avian nucleus isthmi and its relation to hippus. *Journal of Comparative Neurology*, *132*, 589–615. doi:10.1002/cne.901320407

Stacho, M., Letzner, S., Theiss, C., Manns, M., & Güntürkün, O. (2016). A GABAergic tecto–tegmento–tectal pathway in pigeons. *Journal of Comparative Neurology*, 524(14), 2886–2913. doi:10.1002/cne.23999

Swanson, L. W., & Lichtman, J. W. (2016). From cajal to connectome and beyond. *Annual Review of Neuroscience*, *39*, 197–216. doi:10.1146/annurev-neuro-071714-033954

Uchiyama, H. (1989). Centrifugal pathways to the retina: Influence of the optic tectum. *Visual Neuroscience*, *3*, 183–206. doi:10.1017/S0952523800009950

Uchiyama, H., Aoki, K., Yonezawa, S., Arimura, F., & Ohno, H. (2004). Retinal target cells of the centrifugal projection from the isthmo-optic nucleus. *Journal of Comparative Neurology*, *476*, 146–153. doi:10.1002/cne.20225

Uchiyama, H., & Barlow, R. B. (1994). Centrifugal inputs enhance responses of retinal ganglion cells in the japanese quail without changing their spatial coding properties. *Vision Research*, *34*, 2189–2194. doi:10.1016/0042-6989(94)90101-5

Uchiyama, H., & Ito, H. (1993). Target cells for the isthmo-optic fibers in the retina of the Japanese quail. *Neuroscience Letters*, *154*, 35–38. doi:10.1016/0304-3940(93)90165-H

Uchiyama, H., Nakamura, S., & Imazono, T. (1998). Long-range competition among the neurons projecting centrifugally to the quail retina. *Visual Neuroscience*, *15*, 417–423.

Uchiyama, H., Ohno, H., & Kodama, R. (2012). Lesion of the isthmo-optic nucleus impairs target selection for visually guided reaching. *Behavioural Brain Research*, *233*, 359–366. doi:10.1016/j.bbr.2012.05.008

Uchiyama, H., & Stell, W. K. (2005). Association amacrine cells of Ramón y Cajal: Rediscovery and reinterpretation. *Visual Neuroscience*, *22*, 881–891. doi:10.1017/S0952523805226160

Uchiyama, H., & Watanabe, M. (1985). Tectal neurons projecting to the isthmo-optic nucleus in the Japanese quail. *Neuroscience Letters*, *58*, 381–385. doi:10.1016/0304-3940(85)90085-0

Uchiyama, H., Yamamoto, N., & Ito, H. (1996). Tectal neurons that participate in centrifugal control of the quail retina: A morphological study by means of retrograde labeling with biocytin. *Visual Neuroscience*, *13*, 1119–1127. doi:10.1017/S0952523800007768

Ullmann, J. F. P., Moore, B. A., Temple, S. E., Fernández-Juricic, E., & Collin, S. P. (2012). The Retinal Wholemount Technique: A Window to Understanding the Brain and Behaviour. *Brain, Behavior and Evolution*, *79*, 26–44. doi:10.1159/000332802

Vega-Zuniga, T., Marín, G., González-Cabrera, C., Planitscher, E., Hartmann, A., Marks, V., Mpodozis, J., & Luksch, H. (2016). Microconnectomics of the pretectum and ventral thalamus in the chicken (Gallus gallus). *Journal of Comparative Neurology*, *524*, 2208–2229. doi:10.1002/cne.23941

Verhaart, W. J. (1971). Forebrain bundles and fibre systems in the avian brain stem. *Journal für Hirnforschung*, *13*, 39–64.

Wallenberg, A. (1898). Das mediale Opticusbündel der Taube. *Neurologisches Centralblatt*, *17*, 532–537.

Weidner, C., Desroches, A. M., Repérant, J., Kirpitchnikova, E., & Miceli, D. (1989). Comparative study of the centrifugal visual system in the pigmented and glaucomatous albino quail. *Biological Structures and Morphogenesis*, *2*, 89–93.

Weidner, C., Repérant, J., Desroches, A.-M., Miceli, D., & Vesselkin, N. P. (1987). Nuclear origin of the centrifugal visual pathway in birds of prey. *Brain Research*, *436*, 153–160. doi:10.1016/0006-8993(87)91568-X

Wilson, M., & Lindstrom, S. H. (2011). What the bird's brain tells the bird's eye: The function of descending input to the avian retina. *Visual Neuroscience*, *28*, 337–350. doi:10.1017/S0952523811000022

Wilson, M., Nacsa, N., Hart, N. S., Weller, C., & Vaney, D. I. (2011). Regional distribution of nitrergic neurons in the inner retina of the chicken. *Visual Neuroscience*, *28*, 205–220. doi:10.1017/S0952523811000083

Wolf-Oberhollenzer, F. (1987). A study of the centrifugal projections to the pigeon retina using two fluorescent markers. *Neuroscience Letters*, *73*, 16–20. doi:10.1016/0304-3940(87)90023-1

Woodson, W., Reiner, A., Anderson, K., & Karten, H. J. (1991). Distribution, laminar location, and morphology of tectal neurons projecting to the isthmo-optic nucleus and the nucleus isthmi, pars parvocellularis in the pigeon (Columba livia) and chick (Gallus domesticus): A retrograde labelling study. *Journal of Comparative Neurology*, *305*, 470–488. doi:10.1002/cne.903050310

Woodson, W., Shimizu, T., Wild, J.M., Schimke, J., Cox, K., & Karten, H. J. (1995). Centrifugal projections upon the retina: An anterograde tracing study in the pigeon (*Columba livia*). *Journal of Comparative Neurology*, *362*, 489–509. doi:10.1002/cne.903620405

Wylie, D. R. W., Gutiérrez-Ibáñez, C., Pakan, J. M. P., & Iwaniuk, A. N. (2009). The optic tectum of birds: Mapping our way to understanding visual processing. *Candian Journal of Experimental Psychology*, *63*, 328–338. doi:10.1037/a0016826

Yang, G., Millar, T. J., & Morgan, I. G. (1989). Co-lamination of cholinergic amacrine cell and displaced ganglion cell dendrites in the chicken retina. *Neuroscience Letters*, *103*, 151–156. doi:10.1016/0304-3940(89)90567-3

Yonezawa, T., Segawa, T., Mori, H., Campos, P.F., Hongoh, Y., Endo, H., ... Hasegawa, M. (2017). Phylogenomics and morphology of extinct paleognaths reveal the origin and evolution of the ratites. *Current Biology*, *27*, 68–77. doi:10.1016/j.cub.2016.10.029

How to cite this article: Krabichler Q, Vega-Zuniga T, Carrasco D, et al. The Centrifugal visual system of a palaeognathous bird, the Chilean Tinamou (*Nothoprocta perdicaria*). *J Comp Neurol.* 2017;525:2514–2534. https://doi.org/10.1002/cne.24195